

Transfer of organic carbon through marine water columns to sediments – Insights from stable and radiocarbon isotopes of lipid biomarkers

S. G. Wakeham^{1,*} and A. P. McNichol²

¹Skidaway Institute of Oceanography, 10 Ocean Science Circle, Savannah, GA 31411
USA

²National Ocean Sciences Accelerator Mass Spectrometer Facility (NOSAMS), Woods Hole Oceanographic Institution, McLean Laboratory, Mail Stop #8, 266 Woods Hole Road, Woods Hole, MA 02543-1539 USA

Key words: marine sediments, sediment traps, lipid biomarkers, stable carbon isotopes, radiocarbon, Black Sea, Arabian Sea, Ross Sea

*Corresponding author: email stuart.wakeham@skio.usg.edu

23

Abstract

24

Compound-specific ^{13}C and ^{14}C compositions of diverse lipid biomarkers (fatty acids, alkenones, hydrocarbons, sterols, and fatty alcohols) were measured in sinking particulate matter collected in sediment traps and from underlying surface sediments in the Black Sea, the Arabian Sea and the Ross Sea. The goal was to develop a multi-parameter approach to constrain relative inputs of organic carbon (OC) from marine biomass, terrigenous vascular plant, and relict kerogen sources. Using an isotope mass balance, we calculate that marine biomass in sediment trap material from the Black Sea and Arabian Sea accounted for 66-100% of OC, with lower terrigenous (3-8%) and relict (4-16%) contributions. Marine biomass in sediments constituted lower proportions of OC (66-90%), with consequentially higher proportions of terrigenous and relict carbon (3-17% and 7-13%, respectively). Ross Sea data were insufficient to allow similar mass balance calculations. These results suggest that whereas particulate organic carbon is overwhelmingly marine in origin, pre-aged allochthonous terrigenous and relict OC become proportionally more important in sediments, consistent with pre-aged OC being better preserved during vertical transport to and burial at the seafloor than the upper ocean-derived marine OC.

41

42

43

44

45 **1 Introduction**

46 The dynamics of sources, sinks and processes that control burial of organic carbon (OC)
47 in marine sediments have important implications for the global carbon cycle,
48 paleoceanographic reconstructions and understanding climate variability (Berner, 1982;
49 Hedges and Keil, 1995; Burdige, 2007; Zonneveld et al., 2010). Assigning the
50 provenance of sedimentary OC remains a difficult task. Most burial occurs on
51 continental margins where terrigenous material constitutes a significant proportion of the
52 burial flux (Hedges et al., 1997; Burdige, 2005). But even at open ocean locations
53 remote from the continents where marine OC dominates the water column flux via the
54 biological pump, a terrigenous component delivered by long-range aeolian transport
55 (Zafiriou et al., 1995; Gagosian and Peltzer, 1986; Eglinton et al., 2002; Kawamura et al.,
56 2003) is still recognizable in sediments (Prahl et al., 1989; Wakeham et al., 2002;
57 Zonneveld et al., 2010). Myriad biogeochemical and sedimentological processes during
58 transport through the marine water column and at the sediment-water interface affect the
59 quantity and nature of sedimentary OC. Structural characterization of most marine
60 organic matter is incomplete (Hedges et al., 2000; Lee et al., 2004), but it is generally
61 thought that marine OC is more reactive than terrigenous plant and relict sediment OC
62 (Cowie and Hedges, 1984; Wakeham et al., 1997). Even a small fraction of the most
63 recalcitrant relict carbon is amenable to bacterial assimilation (Petsch et al., 2001, 2003;
64 Pearson et al., 2005; Wakeham et al., 2006). Selective enrichment of terrigenous OC in
65 marine sediments over what is observed in the water column may result from differences
66 in the intrinsic reactivity of the organic molecules themselves, protection by degradation-
67 resistant macro-organic matrices and mineral surfaces, or environmental conditions

68 (oxygen availability, oscillating redox, microbial consortia present) (Hedges and Keil,
69 1995; Hedges et al., 2001; Aller, 1994; Wakeham and Canuel, 2006; Burdige, 2007).

70 A suite of geochemical tools are applied to characterize the source(s) and fate of
71 OC in the marine water column and sediments. Elemental compositions and ratios (e.g.,
72 OC/N) are often combined with carbon isotope analyses at the bulk level. Natural
73 abundance stable carbon isotopes ($\delta^{13}\text{C}$) give insight into carbon source, carbon
74 assimilation pathways and carbon flow in marine ecosystems and food webs (Hayes,
75 1993; Fry and Sherr, 1994; Freeman, 2001; Pearson, 2010). Natural-abundance
76 radiocarbon analyses ($\Delta^{14}\text{C}_{\text{OC}}$ or fraction modern f_m) add the dimension of “age” to the
77 character of organic matter and help define the residence time and redistribution of OC
78 (Blair et al., 2003; Ingalls and Pearson, 2005; Griffith et al., 2010). Molecular analyses
79 of biomarkers can distinguish between marine (e.g., sterols, alkenones), terrigenous
80 (plant waxes and lignin phenols) and relict (alkanes with a carbon preference index of ~ 1
81 and often an unresolved complex mixture) materials in the heterogeneous mixture that is
82 sedimentary OC. But biomarker compounds are often present at low concentrations, and
83 extrapolations to bulk OC are formidable. Single-compound (compound-specific)
84 isotope analyses help in this respect because they combine the source-specificity of
85 biomarkers with $\delta^{13}\text{C}_{\text{biomarker}}$ -derived information on carbon flow (Freeman et al., 1990;
86 Hayes, 2001; Freeman, 2001) and $\Delta^{14}\text{C}_{\text{biomarker}}$ -derived ages that indicate mixing of old
87 with modern OC (Eglinton et al., 1997; McNichol and Aluwihare, 2007; Ingalls and
88 Pearson, 2005). Early investigations in the marine water column showed that whereas
89 sinking particulate OC comprised of fresh planktonic detritus has a young radiocarbon
90 age, surface sedimentary OC has older ages of a “pre-aged” and/or relict terrigenous

91 component (Druffel et al., 1996; Wang et al, 1998; Hwang et al., 2010). Compound-
92 specific radiocarbon measurements confirm pre-aged biomarkers in sedimentary OC
93 (review by Ingalls and Pearson, 2005), and compound-class radiocarbon analyses have
94 subsequently shown pre-aged OC in water column particulate matter (Wang et al., 2001;
95 review by McNichol and Aluwihare, 2007). However, to date combined
96 biomarker/stable carbon/radiocarbon studies of marine particulate matter are few (an
97 exception being Ingalls et al., 2006), largely due to sample size limitations.

98 The present investigation attempts to fill this gap. The combination of lipid
99 biomarker composition with molecular stable- and radio-carbon isotopes offers a three-
100 dimensional approach for investigating OC sources and transport and alteration processes
101 in the ocean. In this study, compound-specific stable carbon and radiocarbon isotopes
102 were measured on multiple lipid biomarkers in sinking particulate matter collected in
103 sediment traps and from underlying surface sediments to evaluate the provenance of
104 sedimentary organic matter. Three sets of paired sediment trap-surface sediment samples
105 (POM – particulate organic matter; SOM – sedimentary organic matter) from the Black
106 Sea, Arabian Sea and Ross Sea were investigated as representatives of oceanic regions
107 characterized by widely disparate OC sources and depositional environments. Organic
108 carbon content (%OC), atomic C/N ratios (C/N_(a)), $\delta^{13}\text{C}$ and $\Delta^{14}\text{C}$ of bulk materials and
109 individual biomarkers (fatty acids, hydrocarbons, alkenones, alcohols, and sterols) were
110 measured to identify major molecular and isotopic compositions, and thereby shifts in
111 relative amounts of marine, terrigenous (pre-aged vascular plant-derived with continental
112 residence times of decades to centuries) and relict (derived from eroded ancient
113 sedimentary rocks and petrogenic material) carbon, in POM and underlying SOM.

114 Throughout this discussion it is important to remember that the sediment trap samples are
115 short snap-shots in time (up to 6 months) whereas the surface sediments may represent
116 centuries.

117

118 **2 Materials and Methods**

119 **2.1 Study sites and samples**

120 Paired sediment trap and surface sediment (~0-2 cm) samples from three settings
121 (Fig. 1) were studied: Black Sea (anoxic water column; high biogenic and high
122 terrigenous OC); Arabian Sea (oxygen minimum zone; high biogenic OC, low
123 terrigenous OC); Ross Sea, Antarctica (high biogenic flux, relict continental OC). The
124 choice of these locations was predicated in part on the availability of large amounts of
125 archived sinking particulate matter to facilitate compound-specific radiocarbon analyses.

126

127 **2.1.1 Black Sea**

128 The Black Sea site was in southwestern Black Sea (42°N, 32°E), at station BS of
129 the joint U.S. Turkish/German sediment trap program 50 km north of Asmara and 15 km
130 from the base of the continental slope (Hay and Honjo, 1989; Hay et al., 1990). Anoxic
131 conditions prevail below ~120-150 m water depth (Sorokin, 1983). Underlying
132 sediments contain up to ~6% OC (Ross and Degens, 1974; Premuzic et al., 1982; Calvert
133 et al., 1991). Biogenic and lithogenic particle fluxes and sediment accumulation have
134 been reported by Hay (1987) and Hay et al. (1990). The site is offshore of the rugged
135 Pontic Mountains on the north-Anatolian coastline and the continental margin is
136 particularly steep, typically 6° between 100 and 2000 m depths (Ross et al., 1974).

137 Lithogenic material delivered by the Sarkarya Nehri, Filyos and Kocacay Rivers, usually
138 during winter/spring, is deposited on the shelf, is frequently resuspended by storms, and
139 is subsequently transported off-shore as either surface, mid-water (~150 m depth) or
140 bottom water nepheloid layers and turbidites; a surface plume extending out to the study
141 site is sometimes visible on LANDSAT imagery (Hay, 1987). Sedimentation of
142 lithogenic material out of the water column is enhanced by biogenic material derived
143 from the annual succession of blooms of the coccolithophoride *Emiliania huxleyi* (spring)
144 and pennate diatoms *Rhizosolenia* sp. (summer), producing the characteristic light-dark
145 laminae (varve couplets) of Black Sea sediments (Hay, 1987; Hay et al., 1991). White
146 laminae are comprised almost exclusively of coccolithophores of *E. huxleyi*, whereas
147 dark laminae are predominately terrigenous clay minerals.

148 Sediment trap material (18.5 g dry weight) from the moored BS trap at ~250 m
149 depth under strongly anoxic conditions is a composite of a seven month-long time-series
150 collection (October 1985-April 1986). Trap material was preserved with buffered
151 formalin and stored refrigerated at 4°C. Surface sediment (0-2 cm; 109.7 gdw) was
152 composited from multicores collected at 2200 m water depth during the 1988 Black Sea
153 Expedition (Murray and Izdar, 1989; Hay and Honjo, 1989) at approximately the same
154 location as the trap mooring. Sediments were stored frozen. Radiocarbon dating of
155 sediments near the study site gave a sedimentation rate of 26 cm/kyr (Arthur and Dean,
156 1998). Thus the 0-2 cm sediment interval represents approximately one century.

157

158 **2.1.2 Arabian Sea**

159 Arabian Sea samples were collected at mooring site MS-1 in the northwestern
160 Arabian Sea (Oman Margin) during the U.S. JGOFS Arabian Sea Process Study (ASPS)
161 in 1994-1995 (Smith et al., 1998). MS-1 was approximately 160 km from the Oman
162 coast off Ra's Sharbatat ($17^{\circ}41'N$, $58^{\circ}51'E$) at a water depth of 1445 m. High seasonal
163 productivity during monsoon-driven upwelling enhances export into deep waters where
164 remineralization of sinking organic matter depletes dissolved oxygen down to levels of
165 $\sim 5 \mu M$, producing the world's largest open ocean oxygen minimum zone (OMZ) (Smith
166 et al., 1998). Greater than 50% of the annual particle flux in the central Arabian Sea
167 occurs during the boreal summer southwest monsoon. Biogenic material, primarily
168 diatom-derived, dominates over lithogenic material (Haake et al., 1996; Honjo et al.,
169 1999), but some terrigenous material is delivered to the northwestern Arabian Sea as dust
170 from the Horn of Africa (Somalia and Ethiopia) and from the Arabian Peninsula by
171 strong summer monsoon winds (Ramage et al., 1972; Sirocko and Sarnthein, 1989; Dahl
172 et al., 2005).

173 Sediment trap material (35.5 gdw) was a composite of material collected in time-
174 series traps deployed in the OMZ at ~ 500 and ~ 900 m between May 1995 and January
175 1996, covering the southwest monsoon period (Wakeham et al., 2002). Mercuric
176 chloride was used as a biocide. Upon recovery, trap samples were sealed and stored
177 refrigerated at $4^{\circ}C$. Surface sediments (0-2 cm) were composited (142.7 gdw) from
178 multicores collected in 1995 at the same location as the trap deployment and stored
179 frozen. Passier et al. (1997) have estimated the sedimentation rate for this part of the
180 Oman Margin at 5 cm/kyr; the sediment sample thus represents about 400 years.

181

182 **2.1.3 Ross Sea**

183 The Ross Sea site was in the southwestern Ross Sea where diatoms, primarily
184 *Nitzschia* sp., and *Phaeocystis antarctica*, dominate the phytoplankton community and
185 vertical flux during the austral summer bloom (Arrigo et al., 2002; Dunbar et al., 2003).
186 Sediments are largely biogenic oozes (biogenic silica 10-30%) with low OC (0.1-3%,
187 averaging 1.5%) and negligible biogenic carbonate (Dunbar et al., 1985; 1989).
188 Terrigenous material, primary lithogenics with low OC content, is delivered by glaciers
189 that drain the polar plateau and by aeolian transport from the ice-free Dry Valleys and
190 accounts for 2-25% of the vertical flux through the water column. In the western Ross
191 Sea, ice-rafted debris constitutes ~10% of sediments (Anderson et al., 1984) and aeolian
192 sedimentation (either through sea ice or directly onto the sea surface) could be up to 50%
193 of sediments in nearshore areas with limited glacial ice cover (Bentley, 1979, cited in
194 Dunbar et al., 1989). Nonetheless, sedimentary OC is dominated by biogenic water
195 column sources. Sediments are resuspended, mixed and redistributed within a pervasive
196 nepheloid layer.

197 Ross Sea samples were collected during 1998 cruises of the ROAVERRS
198 (Research on Ocean-Atmosphere Variability and Ecosystem Response in the Ross Sea)
199 program (Dunbar et al., 2003). Trap material (48.2 gdw) came from Gentoo and Adelie
200 time-series traps located at about 76° S, 172 E in the southwestern Ross Sea and
201 deployed ~50 m above the sea floor in 650-m deep water (Dunbar et al., 2003). Trap
202 material was preserved with 3% formalin and stored at 4°C. Surface sediments (515.1
203 gdw) were obtained from box cores (Ohkouchi et al., 2003) and stored frozen.

204 Sedimentation rate determinations for the Antarctic margin often use acid-
205 insoluble organic carbon (AIOC) due to lack of calcareous foraminifera (Domack et al.
206 1989; Licht et al. 1996; Harris et al. 1996; Andrew et al. 1999). DeMaster et al. (1996)
207 reported AIOC-derived sedimentation rates in this region of the Ross Sea at ~4.5 cm/kyr.
208 AIOC-based chronology, however, is complicated by “contamination” by unknown
209 amounts of relict OC (Sackett et al. 1974). To overcome this problem, Ohkouchi et al.
210 (2003) applied compound-specific radiocarbon analysis of sedimentary fatty acids for
211 cores from the Gentoo and Adelie sites and found a 1200-2000 year offset between ages
212 of fatty acids and AIOC. The fatty acid-derived sedimentation rate was 7.5 cm/kyr vs. an
213 AIOC-derived rate of 15 cm/kyr. The sediment sample therefore represents 130-250
214 years of deposition.

215

216 **2.2 Elemental analysis**

217 Freeze-dried and acidified (Hedges and Stern, 1984) trap material (bulk POM)
218 and sediments (bulk SOM) were analyzed for organic carbon (% OC) and total nitrogen
219 (TN) with a Fisons CHN analyzer (Model EA 1108) elemental analyzer.

220

221 **2.3 Lipid analysis**

222 Extraction, cleanup and isolation of fatty acids, hydrocarbons, alcohols and sterols
223 by preparative capillary gas chromatography (PCGC; Eglinton et al., 1996) are outlined
224 in Fig. 2. All laboratory glassware and SiO_2 were precombusted at 500 °C for 8 hr before
225 use. Freeze-dried POM and SOM were Soxhlet-extracted with methylene-
226 chloride:methanol (DCM:MeOH, 2:1 v/v) for 72 hr. Extracts were washed with 5%

227 NaCl solution and solvent lipid extracts (SLEs) were partitioned into DCM, after which
228 the DCM fraction was dried over Na₂SO₄. SLEs were saponified using 0.5 N KOH at
229 100° C for 2 hr, and nonsaponifiable lipids were extracted out of the alkaline mixture
230 with hexane after which the pH was adjusted to <2 with 6N HCl and acids were extracted
231 with hexane. Non-saponifiable lipids were fractionated on 5% deactivated silica gel into
232 a hydrocarbon fraction eluted with hexane, an alkenone fraction eluted with 10%
233 ethylacetate in hexane and an alcohol/sterol fraction eluted with 25% ethylacetate in
234 hexane. Straight-chained hydrocarbons were separated from branched and cyclic
235 hydrocarbons by urea adduction. Alkenones were isolated by sequential silica gel,
236 AgNO₃/silica gel chromatography and urea adduction after Ohkouchi et al. (2005).
237 Alcohols and sterols were acetylated with pyridine and acetic anhydride. Acids were
238 methylated with BF₃:MeOH and the fatty acid methyl esters (FAMEs) were purified on
239 columns of activated SiO₂.

240

241 **2.4 Stable and Radiocarbon Analysis**

242 Isolation of purified individual hydrocarbons, sterol acetates, alcohol acetates and
243 FAMEs was by preparative capillary gas chromatography (PCGC; Eglinton et al., 1996;
244 Wakeham et al., 2006). An HP 5980II GC equipped with an HP 7673 autoinjector, a
245 Gerstel CIS-3 cooled injection system and a Gerstel preparative fraction collector (PFC)
246 was fitted with RTX-1 megabore (60 m x 0.53 mm id x 0.5µm film) capillary column.
247 The GC temperature program was 60°C (1 min), 20°C/min to 160°C, 4°C/min to 300°C
248 and isothermal at 300°C for 20 min. An effluent splitter directed 1% of the column
249 effluent to the FID and the remaining 99% was sent to the zero-dead-volume splitter of

250 the PFC. The PFC was operated at 320°C and U-tube traps were held at room
251 temperature. Purified fractions were checked for purity and quantified by gas
252 chromatography-mass spectrometry (Agilent 6890 gas chromatograph, Agilent 5793
253 mass spectrometer, 30 m x 0.25 mm i.d. J&W DB-5 capillary column). Individual,
254 composited compounds or operational classes were transferred to glass ampules and
255 flame-sealed for isotope analysis.

256 Stable and radio-carbon isotope measurements were made at the National Ocean
257 Sciences Accelerator Mass Spectrometry (NOSAMS) Facility at the Woods Hole
258 Oceanographic Institution. $\delta^{13}\text{C}$ values are reported relative to the VPDB (precision ± 0.2
259 ‰) and $\Delta^{14}\text{C}$ values are reported according to Stuiver and Polach (1977) using the year of
260 sample collection for age correction. Acidified POM and SOM were transferred to pre-
261 combusted Vycor tubes containing CuO and Ag powder. Sample extracts and isolated
262 biomarkers were transferred with solvent to pre-combusted Vycor tubes, and after
263 evaporating the solvent, 100 mg pre-combusted CuO was added to the tube. Samples
264 were combusted to CO₂ at 850°C for 5 hours. After purification and quantification, a
265 split of the CO₂ was analyzed for $\delta^{13}\text{C}$ on a VG Micromass Optima isotope ratio mass
266 spectrometer. The remaining CO₂ was reduced to filamentous graphite over either Fe or
267 Co powder. Radiocarbon analyses of both large and small samples were performed using
268 standard NOSAMS procedures (McNichol et al., 1994; von Reden et al., 1998; Pearson et
269 al., 1998). Processing and combustion blanks of a hydrocarbon fraction isolated from a
270 south Louisiana crude oil had replicate $\Delta^{14}\text{C}$ values between -980 and -998 ‰ (f_m 0.03
271 and 0.001, respectively). Contributions of added methyl carbon derived from methanol
272 in FAMEs and acetyl carbons from acetic anhydride in alcohol and sterol esters were

273 removed by isotopic mass balance (Pearson, 2000; Wakeham et al., 2006). The $\delta^{13}\text{C}$ and
274 $\Delta^{14}\text{C}$ values of carbon in the $\text{BF}_3:\text{MeOH}$ and acetic anhydride reagents were calculated
275 by measuring the $\delta^{13}\text{C}$ and $\Delta^{14}\text{C}$ values of palmitic acid and cholesterol standards and of
276 methylpalmitate and cholesteryl acetate prepared using the same lots of $\text{BF}_3\text{-MeOH}$ and
277 acetic anhydride, respectively, and isolated by PCGC.

278 Several FA had unusually high $\Delta^{14}\text{C}$ values and were not used in subsequent
279 calculations of ranges, means and standard deviations of radiocarbon data (shown in bold
280 italics in Tables 1-3). The reasons for these enrichments are unknown (see Wakeham et
281 al., 2006 for additional discussion). Radiotracers had never been used in the SkIO
282 laboratory that was thoroughly checked for any radiocarbon contamination and crude oil
283 process blanks were free of modern carbon. The most enriched FA (most often but not
284 always 16:0, 18:1 and 18:0) were compounds isolated in the highest concentrations and
285 thus for which larger amounts of carbon were analyzed by AMS rather than the less-
286 abundant compounds. Such enrichments were not systematic, and in several cases
287 replicate AMS analyses from splits of the same isolates were made, but with similar
288 results indicating that any contamination must have occurred prior to or during PCGC
289 workup. However, Levin and Kromer (1997) suggested that the average ^{14}C of
290 atmospheric CO_2 between 1980 and present may have been $\sim 200\text{ \textperthousand}$ whereas analysis of
291 post-bomb sediment from the Santa Monica Basin by Pearson and Eglinton (2000)
292 indicates an average ^{14}C of atmospheric CO_2 around 1960 may have been $\sim 400\text{ \textperthousand}$. Thus
293 while it is not possible to completely rule out incorporation of higher amounts of post-
294 bomb ^{14}C into these biomarkers $\Delta^{14}\text{C}$, other marine biomarkers and bulk OC are not
295 consistent with such a scenario.

296

297 **3 Results and discussion**

298 **3.1 Bulk elemental compositions**

299 Organic carbon contents (%OC) of POM (Fig. 3a) were 8.7 % in the Black Sea
300 (BS), 6.4 % in the Arabian Sea (AS) and 5.5 % in the Ross Sea (RS). Total nitrogen
301 (%TN) contents were 1.1, 0.86, and 0.92 %, respectively, for the BS, AS and RS trap
302 material. Thus atomic C/N ratios were 7.7, 7.4, and 5.9 (Fig. 3b). Sediment %OC and
303 %TN were lower: 1.8, 2.3, and 0.54 % OC for the BS, AS, and RS, respectively; 0.20,
304 0.29, and 0.08 % TN for the BS, AS, and RS, respectively. C/N_(a) ratios for sediments
305 were somewhat higher (9.4, 7.7, 6.5 for BS, AS, and RS, respectively) than for POM.
306 Except for the BS sediment, C/N_(a) ratios of the other trap and sediment samples were
307 sufficiently Redfield-like to indicate the predominance of marine OC. The higher C/N_(a)
308 ratio of the BS sediment suggests a somewhat higher component of terrigenous OC;
309 alternately the higher C/N_(a) ratio could result from preferential loss of nitrogen during
310 degradation of OC, but this process is likely limited by the anoxic water column of the
311 BS.

312

313 **3.2 Bulk stable carbon isotopes**

314 BS and AS POM $\delta^{13}\text{C}_{\text{OC}}$ values were typical for marine dominated OC: $-22.9\text{ \textperthousand}$
315 and $-22.4\text{ \textperthousand}$ for the Black Sea and Arabian Sea, respectively (Fig. 4a). $\delta^{13}\text{C}_{\text{OC}}$ values for
316 the corresponding SOM were both slightly more negative (BS $-25.3\text{ \textperthousand}$) and more
317 positive (AS $-20.8\text{ \textperthousand}$) compared to the corresponding POM. The ^{13}C -depletion in the
318 BS sediment could reflect a greater long-term/time-averaged terrigenous C₃-plant OC

319 component (Collister et al., 1994; Conte and Weber, 2002; Chikaraishi et al., 2004) from
320 the heavily wooded Anatolian coast than was present in the short-term trap sample. The
321 relative enrichment of the AS sediment compared to the trap material could be the result
322 of the addition of isotopically-enriched aeolian-transported OC derived from C₄-grasses
323 in the arid Horn of Africa and Arabian Peninsula (Parker et al., 2004; Dahl et al., 2005),
324 but again sampling time-scales for trap and sediment are different.

325 The Ross Sea is a very different environment. Both POM and SOM had $\delta^{13}\text{C}_{\text{OC}}$
326 values of -27.9 ‰ , significantly isotopically-depleted compared to BS and AS samples.
327 Algal biomass at high latitudes is typically depleted in ^{13}C relative to algal OC at lower
328 latitudes (Rau et al., 1991a,b; DeHairs et al., 1997; Freeman, 2001). Several factors may
329 be involved in this differential photosynthetic isotope fractionation, including high algal
330 growth rates, higher dissolved CO₂ concentrations associated with low seawater
331 temperatures, and carbon assimilation mechanism (Rau et al., 1991a,b; DeHairs et al.,
332 1997; Freeman, 2001). In the open southwest Ross Sea, diatom and *Phaeocystis* biomass
333 is -28 ‰ to -27 ‰ (Villinski et al., 2000). Sea-ice algae would add ^{13}C -enriched OC
334 (Gleitz et al., 1996; Gibson et al., 1999; Villinski et al., 2000) but is not a significant
335 source of algal OC at the study site. Antarctic kerogen and coal have $\delta^{13}\text{C}_{\text{OC}}$ values of $-$
336 22 ‰ and -24 ‰ , respectively (Sackett, 1986; Burkins et al., 2000), and soils from the
337 McMurdo Dry Valley region have a wide range of $\delta^{13}\text{C}_{\text{OC}}$ values, $\sim-30\text{ ‰}$ to $\sim-18\text{ ‰}$
338 (and C/N(a) of 11 ± 4) (Burkins et al., 2000).

339 Solvent lipid extracts (SLE) would help bridge the gap between bulk OC and
340 individual biomarkers. In all three sample pairs, SLE's were depleted by up to 4 ‰ in
341 ^{13}C compared with the respective bulk OC's (Fig. 4b). $\delta^{13}\text{C}_{\text{SLE}}$ values for both traps and

342 sediments followed the same trend among samples as $\delta^{13}\text{C}_{\text{OC}}$: $\delta^{13}\text{C}_{\text{AS-SLE}} > \delta^{13}\text{C}_{\text{BS-SLE}} >$
343 $\delta^{13}\text{C}_{\text{RS-SLE}}$. Lipids are a relatively abundant fraction of OC in phytoplankton and
344 zooplankton but are usually only a few percent of OC in particulate matter and sediments
345 (Wakeham et al., 1997; Wang and Druffel, 2001). They would thus not be major
346 contributors to particulate and sedimentary $\delta^{13}\text{C}_{\text{OC}}$ compared to more abundant proteins
347 and carbohydrates that are ~4-6 ‰ enriched in ^{13}C relative to lipids. Intra-class
348 comparisons of isotopic compositions in marine systems are few. A study of $\delta^{13}\text{C}$ of
349 particulate and sedimentary OC in the northeast Pacific and Southern Oceans found that
350 total hydrolysable amino acids (THAA) and total carbohydrates (TCHO) in
351 phytoplankton, zooplankton and sediments were enriched in ^{13}C by about ~2 ‰ and ~3
352 ‰, respectively, relative to OC whereas lipids were depleted ~4 ‰ relative to OC (Wang
353 et al., 1998; Wang and Druffel, 2001).

354

355 **3.3 Bulk radiocarbon isotopes**

356 Radiocarbon isotopic values for BS and AS trap OC ($\Delta^{14}\text{C}_{\text{OC}}$) were 21 ‰ and 14
357 ‰ and for BS and AS sediments were -199 ‰ and -138 ‰, respectively (Fig. 4c and
358 Tables 1-3 which also lists radiocarbon ages and fraction (%) modern, f_{m}). RS POC and
359 SOC were depleted in ^{14}C (-208 ‰ and -355 ‰, respectively) relative to the two other
360 sites. $\Delta^{14}\text{C}_{\text{DIC}}$ values for pre-bomb and post-bomb mixed-layer DIC (dissolved inorganic
361 carbon) in the Black Sea are ~-70 ‰ and 100 ‰, respectively (Jones and Gagnon, 1994)
362 and in the AS are ~-60 ‰ and ~70 ‰ (Stuiver and Östlund, 1983; Sounthor et al., 2002);
363 these values determine the $\Delta^{14}\text{C}$ of autochthonous marine biomass. Pre-bomb and post-
364 bomb $\Delta^{14}\text{C}_{\text{DIC}}$ values in the Ross Sea are lower than elsewhere, -130 ‰ and -100 ‰,

365 respectively (Berkman and Forman 1996; Gordon and Harkness 1992; Hall et al., 2010).
366 In the AS and RS, upwelling of ^{14}C -depleted deep-waters and the short residence time of
367 surface waters lead to the high surface-water reservoir ages (~700 yr and ~1100 yr for AS
368 and RS, respectively vs. ~400 yr for open ocean locations, including the BS; Stuiver and
369 Braziunas, 1993; Siani et al., 2000; Southon et al., 2002; Key, 2004; Hall et al., 2010).
370 Thus trap OC displayed post-bomb signatures for their respective regions but additionally
371 contained older carbon, especially in the Ross Sea. Sediments contained significant
372 contributions of old carbon, and corrected $^{14}\text{C}_{\text{OC}}$ -ages (Tables 1-3) are significantly older
373 than estimated geological ages (100-400 yr, admittedly based on $^{14}\text{C}_{\text{OC}}$ -derived
374 sedimentation rates).

375 Trap and sediment SLE's for the BS and RS had higher $\Delta^{14}\text{C}_{\text{SLE}}$ values than
376 corresponding $\Delta^{14}\text{C}_{\text{OC}}$ values (Fig. 4d): $\Delta^{14}\text{C}_{\text{SLE}}$ values were -96 ‰ and -150 ‰ for BS
377 trap and sediment, respectively; -154 ‰ and -211 ‰ for RS trap and sediment. That the
378 BS and RS trap lipid fractions had lower $\Delta^{14}\text{C}_{\text{SLE}}$ values than $\Delta^{14}\text{C}_{\text{OC}}$ values indicates that
379 some old carbon was extractable (e.g., plant waxes and petroleum hydrocarbons). But
380 the higher sediment $\Delta^{14}\text{C}_{\text{SLE}}$ values than sediment $\Delta^{14}\text{C}_{\text{OC}}$ suggested that residual OC
381 remaining after solvent extraction must be, by extension, still older, such as non-
382 extractable kerogen, especially in the RS sediment. On the other hand, $\Delta^{14}\text{C}_{\text{SLE}}$ of the AS
383 trap material was enriched (66 ‰) compared to $\Delta^{14}\text{C}_{\text{OC}}$ value, but the sediment was
384 depleted (-173 ‰) relative to its $\Delta^{14}\text{C}_{\text{OC}}$ value. Thus solvent extraction of the AS trap
385 material released a greater proportion of fresh, young algal lipid into the SLE but
386 extraction of the sediment recovered an SLE with a greater proportion of older lipid. In
387 the only other reports to our knowledge that measured $\Delta^{14}\text{C}_{\text{SLE}}$ (Wang et al., 1998; Wang

388 and Druffel, 2001), plankton and sedimentary lipids in the northeastern Pacific and
389 Southern Ocean were similar to or lower than, respectively, $\Delta^{14}\text{C}$ of total OC. Lipids,
390 THAA and TCHO all had similar $\Delta^{14}\text{C}$ values in plankton, but in sediments lipids usually
391 had lower $\Delta^{14}\text{C}$ signatures than THAA and THCO.

392

393 **3.4 Biomarker molecular compositions**

394 Biomarker analyses focused on fatty acids, alkenones, fatty alcohols, sterols, and
395 hydrocarbons (Figs 5-7). In the following discussion, the operational distinction is made
396 between biomarkers of marine origin (hereafter termed “marine OC”), those derived from
397 pre-aged terrestrial vascular plants (“terrigenous OC”) and compounds originating from
398 eroded ancient sediment or petrogenic sources (“relict OC”). In all POM samples, short-
399 chain C₁₄-C₂₄ *n*- and methyl-branched *iso*- and *anteiso*-C₁₅ and C₁₇ compounds of marine
400 biomass dominated fatty acid distributions (Volkman, 2006). Long-chain, even-carbon
401 number predominant C₂₄-C₃₀ terrestrial vascular plant *n*-fatty acids were ~10-fold less
402 abundant. Sediments contained similar fatty acid distributions but with higher relative
403 abundances (but still ~3-5-fold less abundant) of long-chain compounds. Long-chain
404 C₃₇-C₃₉ alkenones derived from the haptophyte, *Emiliania huxleyi* (Volkman et al.,
405 1980), were abundant in BS (where coccoliths of *E. huxleyi* constitute the light laminae)
406 and AS traps and sediments, but absent from the RS. Low levels of hydrocarbons, a mix
407 of C₁₅-C₃₆ *n*-alkanes and an unresolved complex mixture (UCM) in the C₁₄ –C₂₂ carbon
408 number range were present in BS and AS samples at levels ~10-fold lower than fatty
409 acids; none above blanks were detected in the RS. Short-chain *n*-alkanes (C₁₆ –C₂₂)
410 showed no odd-over-even carbon number predominance (CPI ~1) and were underlain by

411 an unresolved complex mixture (UCM), whereas long-chain *n*-alkanes (C₂₅ – C₃₁) were
412 odd-carbon predominant (CPI > 5). C₂₅-highly branched isoprenoid (HBI) alkenes of
413 diatom origin were the dominant hydrocarbons in AS POM but were only minor
414 components in BS POM and sediments and AS sediments. No hydrocarbons (above
415 blanks) were detected in RS samples. All POM samples contained abundant *n*-
416 hexadecanol (16 ROH, assumed derived primarily from zooplankton wax esters) and C₂₇-
417 C₃₀-Δ⁵, Δ^{5,22}, Δ^{5,24(28)} sterols [e.g., cholest-5-en-3β-ol (cholesterol), abbreviated as 27Δ⁵;
418 24-methylcholesta-5,22-dien-3β-ol, 28Δ^{5,22}; 24-methylcholesta-5,24(28)-dien-3β-ol,
419 28Δ^{5,24(28)}; and in the BS, a significant amount of 4,23,24-trimethylcholest-22-en-3β-ol
420 (dinosterol), 30Δ²²], all of marine origin (Volkman, 2006). POM contained only low
421 amounts of even-carbon number predominant C₂₄-C₃₀ *n*-alcohols produced by vascular
422 plants, but sediments contained higher abundances of terrestrial *n*-alcohols than sterols.
423

424 **3.5 Biomarker isotopic compositions**

425 PCGC isolation for compound-specific isotope analyses targeted the most
426 abundant biomarkers of marine, terrigenous plant and relict origins. Short-chain *n*-fatty
427 acids (C₁₄-C₂₄, abbreviated as 14:0 FA, etc), C₃₇+C₃₈-alkenones, a short-chain *n*-fatty
428 alcohol [16ROH (*n*-hexadecanol)] and sterols [cholest-5-en-3β-ol (cholesterol),
429 abbreviated as 27Δ⁵; 24-methylcholesta-5,22-dien-3β-ol, 28Δ^{5,22}; and 4,23,24-
430 trimethylcholest-22-en-3β-ol (dinosterol), 30Δ²²], were designated as marine biomarkers.
431 Long-chain even-carbon number *n*-acids (C₂₆-C₃₀) and *n*-alcohols (C₂₄-C₂₈) and long-
432 chain odd-carbon numbered *n*-alkanes (C₂₇, and C₂₉) were tagged as terrigenous, vascular
433 plant markers; in some cases the long-chain fatty acids could be isolated individually but

434 in other cases composites (e.g. C₂₄+C₂₆+C₂₈ fatty acids) were required. Long-chain even-
435 carbon numbered *n*-alkanes (composed C₂₄+C₂₆+C₂₈) and, in the AS sediment, short-
436 chain C₁₅+C₁₆+C₁₇+C₁₈ alkanes (and including some unresolved complex mixture that
437 could not be removed) were used as relict markers since these alkanes are not abundant in
438 marine or terrestrial biomass. As will be shown below, using long-chain *n*-alkanes as
439 either terrigenous plant or relict markers is problematic because in the present samples
440 there is overlap between odd- vs even-chain lengths and plant vs. relict sources. Thus it
441 is possible that long-chain *n*-alcohols, if present in sufficient abundances, may represent
442 the best “terrigenous” biomarkers since they would have neither modern marine (major
443 alcohols in wax esters are C₁₆ and C₁₈; Wakeham, 1982) nor relict sources. Highly
444 branched C₂₅ alkenes (HBI) of diatom origin (Belt et al., 2000) were the most abundant
445 hydrocarbons in AS trap material, less so in AS sediments, but they were underlain by a
446 UCM that could not be removed, thus yielding unrealistically ¹⁴C depleted results. In the
447 RS POM and SOM, only fatty acids, 16 ROH, and sterols (cholest-5-en-3 β -ol and 24-
448 methylcholesta-5,22-dien-3 β -ol) could be isolated. Stable carbon and radiocarbon
449 isotope results were weighted according to their abundance within each sample to give
450 means for each of the three sources (marine, terrigenous, and relict) that are designated
451 below as $\delta^{13}\text{C}_M$ and $\Delta^{14}\text{C}_M$, $\delta^{13}\text{C}_T$ and $\Delta^{14}\text{C}_T$, and $\delta^{13}\text{C}_R$ and $\Delta^{14}\text{C}_R$.

452

453 3.5.1 Black Sea

454 For the Black Sea POM, short-chain fatty acids, long-chain alkenones, and sterols
455 had $\delta^{13}\text{C}$ values between $-26.1\text{ \textperthousand}$ to $-23.2\text{ \textperthousand}$ (Fig. 8a and Table 1), generally 1-4 \textperthousand
456 more ¹³C-depleted than bulk POM ($-22.9\text{ \textperthousand}$). Interestingly, alkenones were the most

457 ^{13}C -depleted of this group. Overall these “marine” biomarkers had an abundance
458 weighted average $\delta^{13}\text{C}_M$ of $-25.3 \pm 1.1 \text{‰}$ (Table 4), typical for marine lipids.
459 Radiocarbon values for the marine biomarkers (excluding the highly ^{14}C -enriched 18:1
460 fatty acid outlier at 288 ‰) ranged from 65 ‰ to 146 ‰, giving $\Delta^{14}\text{C}_M$ of $92 \pm 28 \text{‰}$,
461 considerably enriched in ^{14}C relative to bulk POM ($\Delta^{14}\text{C}_{\text{OC}} -199 \text{‰}$) (Fig. 8b). Long-
462 chain even-carbon number acids and alcohols and odd-carbon number alkanes had $\delta^{13}\text{C}$
463 values ranging from -30.1‰ to -27.0‰ , yielding a mean $\delta^{13}\text{C}_T -28.7 \pm 1.6 \text{‰}$, roughly
464 3‰ depleted in $\delta^{13}\text{C}$ compared to marine lipids. Terrigenous markers had a much greater
465 range of $\Delta^{14}\text{C}$ values (1 ‰ for the fatty acids, -44‰ for the alcohols, and -181‰ for the
466 alkanes) but a mean $\Delta^{14}\text{C}_T$ of $-53 \pm 60 \text{‰}$. It is possible that some fraction of the long-
467 chain fatty acids are zooplankton (wax ester) derived young carbon whereas the long
468 chain alkanes may contain a relict component. Thus the long-chain alcohols may
469 represent the best “terrigenous” biomarkers since they would have neither modern marine
470 (major alcohols in wax esters are C₁₆ and C₁₈; Wakeham, 1982) nor relict sources with a
471 $\Delta^{14}\text{C}$ of -1000‰ . The single sample of “relict” biomarkers isolated by PCGC was a
472 composite of C₂₄+C₂₆+C₂₈ *n*-alkanes that had a $\delta^{13}\text{C}_R$ of $-29.3 \pm 0.2 \text{‰}$ and a $\Delta^{14}\text{C}_R$ of $-$
473 $677 \pm 10 \text{‰}$; this $\Delta^{14}\text{C}$ value probably also reflects a mix of moderately pre-aged
474 terrigenous ($\Delta^{14}\text{C}$ of -44‰ might be reasonable if the alcohols are a good representative
475 of terrigenous OC) and radiocarbon-dead ($\Delta^{14}\text{C}_R$ of -1000‰) relict carbon.

476 Marine biomarkers in the BS sediment had $\delta^{13}\text{C}$ values ranging from -31.9‰ to
477 -26.0‰ (mean $\delta^{13}\text{C}_M -28.8 \pm 1.1 \text{‰}$), about 2.5 ‰ depleted in ^{13}C relative to both BS
478 bulk SOM (-25.3‰) and the marine group of BS POM (also -25.3‰). Radiocarbon
479 contents of marine biomarkers ranged from -46‰ to 75‰ (mean $\Delta^{14}\text{C}_M 2 \pm 44 \text{‰}$,

480 excluding 16:0 at 214 ‰ and 18:0 at 374 ‰), considerably enriched in ^{14}C relative to
481 bulk POM ($\Delta^{14}\text{C}_{\text{OC}} -199$ ‰) but depleted in ^{14}C compared to marine biomarkers in BS
482 POM. Terrigenous biomarkers displayed $\delta^{13}\text{C}$ values between -31.9 ‰ to -29.7 ‰
483 (mean $\delta^{13}\text{C}_{\text{T}} -30.5 \pm 0.65$ ‰). Thus although there was a considerable overlap in $\delta^{13}\text{C}$
484 values for marine and terrigenous groups, concentration weighting yielded an offset of \sim
485 2 ‰ as would be expected. Plant-wax alkanes (C₂₇ and C₂₉) and alcohols (C₂₄ and C₂₆)
486 were strongly depleted in $\Delta^{14}\text{C}$ relative to the marine lipids (range -231 ‰ to -100 ‰),
487 with a mean $\Delta^{14}\text{C}_{\text{T}}$ of -171 ± 58 ‰. Long-chain even-carbon numbered [C₂₄+C₂₆+C₂₈]
488 alkanes had a $\delta^{13}\text{C}$ value of -29.3 ‰ and a $\Delta^{14}\text{C}_{\text{R}}$ of -609 ‰, again suggesting they are
489 pre-aged but not exclusively relict. A similar spread in $\delta^{13}\text{C}$ and $\Delta^{14}\text{C}$ values for marine,
490 vascular plant and relict hydrocarbon biomarkers had been previously reported for Black
491 Sea and Arabian Sea sediments (Eglinton et al., 1997).

492

493 **3.5.2. Arabian Sea**

494 The marine biomarkers in the AS trap POM had $\delta^{13}\text{C}$ values between -27.1 ‰
495 and -16.7 ‰ (mean $\delta^{13}\text{C}_{\text{M}} -23.5 \pm 2.5$) and $\Delta^{14}\text{C}$ contents ranging from -91 ‰ to 111 ‰
496 (Fig. 9a and b and Table 2) (mean $\Delta^{14}\text{C}_{\text{M}} -67 \pm 40$ excluding C_{14:0} at 178 ‰ and HBI
497 alkenes at -514 ‰). The negative $\Delta^{14}\text{C}$ value for the HBI alkenes is due inclusion of a
498 UCM which could not be removed. The only vascular plant compounds in the AS trap in
499 sufficient quantity for AMS analysis were analyzed as a composite of [C₂₇+C₂₉] *n*-
500 alkanes, giving a $\delta^{13}\text{C}_{\text{T}}$ of -28.4 ‰ and a $\Delta^{14}\text{C}_{\text{T}}$ of -320 ‰. The single sample of
501 [C₂₄+C₂₆+C₂₈] *n*-alkanes gave a $\delta^{13}\text{C}_{\text{R}}$ of -28.5 ± 0.2 ‰ and a $\Delta^{14}\text{C}_{\text{R}}$ of -731 ± 14 ‰.

502 The $\delta^{13}\text{C}$ values for marine biomarkers in AS sediments ranged from -26.8 ‰ to
503 -18.2 ‰ ($\delta^{13}\text{C}_M$ mean $-24.5 \pm 2.1\text{ ‰}$), and $\Delta^{14}\text{C}$ ranged from 104 to -171 ‰ ($\Delta^{14}\text{C}_M$ –
504 $59 \pm 60\text{ ‰}$, excluding 18:0 FA at 190 ‰ and HBI alkenes at -256 ‰). Vascular plant
505 [C₂₆+C₂₈+C₃₀] *n*-alcohols had a $\delta^{13}\text{C}$ value of -24.1 ‰ and a $\Delta^{14}\text{C}$ value of $-113 \pm 13\text{ ‰}$
506 and [C₂₇+C₂₉] *n*-alkanes displayed a $\delta^{13}\text{C}$ value of -27.7 ‰ and a $\Delta^{14}\text{C}$ value of $-430 \pm$
507 11 ‰ . Together, the terrigenous biomarkers had a concentration weighted $\delta^{13}\text{C}_T$ value of
508 $-27.7 \pm 0.20\text{ ‰}$ and a $\Delta^{14}\text{C}_T$ of $-270 \pm 110\text{ ‰}$. Two groups of *n*-alkanes in AS sediments
509 could be assigned to relict sources. Short-chain [C₁₄+C₁₅+C₁₆+C₁₇] alkanes and the UCM
510 under this group of homologs had a $\delta^{13}\text{C}$ value of -29.4 ‰ and a $\Delta^{14}\text{C}$ value of -887 ‰ .
511 Long-chain [C₂₄+C₂₆+C₂₈] *n*-alkanes had a $\delta^{13}\text{C}$ value of -27.7 ‰ and a $\Delta^{14}\text{C}$ value of –
512 430 ‰ . Thus $\delta^{13}\text{C}_R$ and $\Delta^{14}\text{C}_R$ for the AS sediments would be $-28.4 \pm 0.2\text{ ‰}$ and -879
513 $\pm 45\text{ ‰}$, respectively.

514

515 **3.5.3. Ross Sea**

516 Ross Sea POM and SOM contained only marine-derived fatty acids (here C₂₆ is
517 considered marine assuming the absence of much terrigenous FA input to the RS) and
518 alcohols/sterols in sufficient abundance for compound-specific isotopic analysis. In
519 keeping with a ¹³C isotope depletion in high latitude regions, noted above, fatty acids had
520 $\delta^{13}\text{C}$ values ranging from -35.3 to -31.7 ‰ and alcohols/sterols values ranging from –
521 35.4 to -31.8 ‰ (Fig. 10a and Table 3), together giving a mean $\delta^{13}\text{C}_M$ of $-33.3 \pm 1.8\text{ ‰}$.
522 Radiocarbon contents ranged from -216 to -100 ‰ , with the alcohols/sterols slightly
523 depleted relative to the fatty acids, for a $\Delta^{14}\text{C}_M$ $-155 \pm 47\text{ ‰}$ (Fig. 10b).

524 Fatty acids and sterols/alcohols in RS sediments had $\delta^{13}\text{C}$ values ranging from –
525 36.6 to –31.7 ‰ and –34.3 to –33.0 ‰, respectively, for a mean $\delta^{13}\text{C}_M$ of -34.3 ± 1.9 ‰.
526 Radiocarbon contents of fatty acids from RS sediments were more variable than for RS
527 POM, with values ranging from –302 to –83 ‰. Sterols from RS sediments were very
528 unchanged from sterols in POM with $\Delta^{14}\text{C}$ values between –202 and –178 ‰ for sterols.
529 Overall this gave a mean $\Delta^{14}\text{C}_M$ of -163 ± 77 ‰, also essentially the same as for $\Delta^{14}\text{C}_M$
530 of the trap material.

531

532 **3.6 The provenance of POM and SOM in the Black Sea and Arabian Sea**

533 Concentration-weighted isotope values (Table 4) can be used to constrain the
534 ranges of isotopic compositions of marine, terrigenous and relict biomarkers, and by
535 extension organic carbon, in Black Sea and Arabian Sea POM and SOM. Neither
536 terrigenous nor relict biomarkers could be isolated from the Ross Sea in sufficient
537 quantities for AMS analyses. Overall, $\delta^{13}\text{C}_M > \delta^{13}\text{C}_T \sim \delta^{13}\text{C}_R$ and $\Delta^{14}\text{C}_M > \Delta^{14}\text{C}_T >>$
538 $\Delta^{14}\text{C}_R$ (Fig. 11). Furthermore, SOM biomarkers were generally ^{13}C -depleted and ^{14}C -
539 depleted relative to their corresponding POM samples, indicative of higher proportions of
540 ^{13}C depleted but older, pre-aged OC in sediments. The range of $\delta^{13}\text{C}_R$ was relatively
541 small compared to $\delta^{13}\text{C}_M$ and $\delta^{13}\text{C}_T$ of POM and SOM, but the span of $\Delta^{14}\text{C}_R$ values was
542 quite large since the odd carbon number hydrocarbons constituting these groups are a mix
543 of old but not radiocarbon “dead” terrigenous vascular plant ($\Delta^{14}\text{C}$ values similar to
544 average $\Delta^{14}\text{C}_T$ values) and truly relict ($\Delta^{14}\text{C}=1000$ ‰) OC.

545 The relative contributions of marine, pre-aged terrigenous, and relict OC (f_M, f_T ,
546 and f_R) to sediment trap material and sediments can be estimated in the Black, Arabian,

547 and Ross Seas using an isotopic mass balance. Plots of $\delta^{13}\text{C}_{M,T,R}$ vs. $\Delta^{14}\text{C}_{M,T,R}$ in both the
 548 sediment traps and sediment (Fig. 11) show significantly different values for the
 549 radiocarbon content of the different carbon pools but relatively small differences in the
 550 stable isotopic content in the Black and Arabian Seas and in the Ross Sea sediments. The
 551 small differences in $\delta^{13}\text{C}$ coupled with significant error make it difficult to use the stable
 552 isotopic composition as a discriminating factor in determining the sources of the bulk
 553 material. However, the large differences observed in the $\Delta^{14}\text{C}$ values make it possible to
 554 use these data to constrain the relative amounts of relict, terrestrial and marine
 555 components.

556 For each sample, there is a $\Delta^{14}\text{C}$ value assigned to the bulk SLE, fresh marine,
 557 fresh terrestrial and a relict/terrestrial mix. Bulk material is assumed to be a mixture of
 558 fresh marine and other “added” material, where the added material refers to the fresh
 559 terrestrial and relict/terrestrial mix. Given this, we can derive the relative amounts of
 560 marine and “added” material.

$$561 \quad I = f_M + f_{added} \quad (1)$$

$$562 \quad \Delta^{14}\text{C}_{bulk} = f_M (\Delta^{14}\text{C}_{mar}) + f_{added} (\Delta^{14}\text{C}_{added}) \quad (2)$$

563 Solving this equation for f_{added}

$$564 \quad f_{added} = \frac{\Delta^{14}\text{C}_{bulk} - \Delta^{14}\text{C}_M}{\Delta^{14}\text{C}_{added} - \Delta^{14}\text{C}_M} \quad (3)$$

565 The value of $\Delta^{14}\text{C}_{added}$ can range from that for relict material (-1000 ‰) to that of
 566 the bulk material. Using this information, we can calculate the relative amounts of
 567 marine and “added” material as a function of the $\Delta^{14}\text{C}$ of the “added” material. Further,
 568 we can combine the radiocarbon value measured on the terrestrial portion with the value

569 of truly relict material to calculate how much of the “added” material might come from
570 fresh terrestrial material using the equations below.

571
$$f_{added} = f_T + f_R \quad (4)$$

572
$$\Delta^{14}\text{C}_{added} = f_T(\Delta^{14}\text{C}_T) + f_R(\Delta^{14}\text{C}_R) \quad (5)$$

573 Truly relict material has a $\Delta^{14}\text{C}$ value of -1000‰ and fresh terrigenous material
574 has the values determined in this study ($\Delta^{14}\text{C}_T$, Table 5). As stated earlier, the measured
575 value of $\Delta^{14}\text{C}_R$ appears to be a mixture of truly relict material and terrigenous material
576 with a suite of ages. If we assume that the value we measured for “relict” material (Table
577 5) is a good representation of $\Delta^{14}\text{C}_{added}$, then we have a unique solution to the mass
578 balance. This solution is indicated by the vertical lines in Figure 12 and the values listed
579 in Table 5. Using this model, we force ourselves to an extreme situation where all the
580 “added” material is either vascular or totally dead. Thus, the relative fractions of
581 terrestrial and relict material must be considered maximum and minimum values,
582 respectively.

583 For the calculations, concentration weighted $\delta^{13}\text{C}_M$, $\delta^{13}\text{C}_T$, $\delta^{13}\text{C}_R$, $\delta^{13}\text{C}_B$, $\Delta^{14}\text{C}_M$,
584 $\Delta^{14}\text{C}_T$ and $\Delta^{14}\text{C}_B$ values listed in Table 4 were used. The relative fractions of marine,
585 terrestrial and relict material (f_M , f_T , and f_R) as a function of $\Delta^{14}\text{C}_{added}$ are shown in Fig.
586 12. It is most likely that the marine component is dominant in both the trap and sediment
587 samples, although the possible values range from >80 to 0%. Fresh vascular material can
588 account for 0 up to almost 100%. The amount of relict material is constant at a low
589 proportion, ranging from 0 to < 20% in both the trap and sediments. In the AS, the
590 marine component is dominant in both the trap and sediments; the trap data indicate that
591 there can be virtually no relict or vascular material input to this sample, while the

592 sediment data suggest that up to 30% of the material may come from either relict or
593 vascular sources. In the RS sediment, marine material dominates in almost all instances,
594 with possible values ranging from 90 to 30%. Relict material can account for >10 to 0%
595 and vascular from 0 to <70%.

596 In the Black Sea and Arabian Sea cases here, it is likely that the marine
597 component contributes the most material because a marine biogenic flux dominates at
598 both sites. No comparable combined biomarker, ^{13}C , and ^{14}C studies of POM at other
599 sites exist to our knowledge. But the high amounts of marine OC in the Black Sea and
600 Arabian Sea sediments contrasts with other environments where similar biomarker-
601 isotopic mass balances have been made, although using a narrower range of biomarkers.
602 In nearshore sediments on the northern California Margin off the high-energy Eel River
603 that erodes ancient sedimentary rocks in its watershed (Blair et al., 2003), fractional
604 contributions from marine, terrestrial and relict components were estimated at 0-10, 50-
605 75 and 30-50 % of total OC (Drenzek et al, 2009). On the Washington Margin off the
606 lower-energy Columbia River, marine, terrestrial and relict OC contribute 2, 89-95 and 3-
607 9 % of bulk sedimentary OC (Feng et al., 2013). Sediments in the Beaufort Sea had f_M, f_T
608 and f_R values of 13-27, 36-42, and 34-37%, respectively, with the elevated f_R values
609 consistent with the well-defined petrogenic signature of *n*-alkanes and polycyclic
610 aromatic hydrocarbons in Mackenzie River and Beaufort Sea sediments (Yunker et al.,
611 1993, 2002). For surface sediments in the southwest Black Sea near our study site,
612 Kusch et al (2010) estimate a f_R of ~18% of TOC. In the Santa Monica Basin of the
613 California Borderlands, 80-87% of the *n*-alkanes were of terrigenous plant origin whereas
614 up to 20% of the alkanes were derived from petroleum or shales (Pearson and Eglinton,

615 2000), but since alkanes are not abundant in most marine biota, no estimation of the
616 marine component was made.

617 For the Black Sea, the graphs for the relative contributions look similar for both
618 the trap and sediment samples. A strict interpretation of these results suggests that there
619 is a greater relative amount of non-marine material in the sediment trap than in the
620 sediments themselves. Given the limitations of our data set, we believe that it is more
621 likely that the relative amounts of material are actually very similar. This is somewhat
622 surprising for two reasons. First, under a differential degradation/preservation case
623 (Wakeham and Canuel, 2006), a more labile component of marine OC would be
624 selectively degraded as POM moved between the trap depths and the surface sediments,
625 leaving behind increased proportions of selectively preserved, more refractory
626 terrigenous and relict components in sediments. Alternately, lateral advection of
627 terrigenous and relict OC below the trap depths either by mid-depth or bottom currents
628 might simply allow this pre-aged material to bypass the traps to be deposited directly on
629 the sediments. At the Black Sea site, advective transport of continental material
630 containing terrigenous and relict carbon to the study site is likely via surface, mid-water
631 (~150 m depth) or bottom water nepheloid layers and turbidites. Surface and mid-water
632 plumes moving offshore could carry some continental material to the shallow (~250 m)
633 sediment trap. But a greater amount of terrigenous and relict carbon might, after
634 temporary storage on the narrow continental shelf, be remobilized to move laterally down
635 the steep continental slope under the trap. This type of advective remobilization of pre-
636 aged material is well documented at other locations for both marine derived alkenones
637 (e.g., Ohkouchi et al., 2002; Mollenhauer et al., 2003) and terrigenous/relict OC (e.g.,

638 Aller et al., 2004; Mead and Goñi, 2006; Mollenhauer and Eglinton, 2007; Kusch et al.,
639 2010; Hwang et al., 2010). Aeolian transport of leaf wax OC and petrogenic OC to the
640 sediments of the central Black Sea have been reported (Wakeham 1996; Eglinton et al.,
641 1997), but the importance of aeolian delivery to the southwestern Black Sea is unknown.
642 Nonetheless, a small leaf wax/petrogenic signal was detected in the trap POM. Because
643 the trap was already deployed within the anoxic zone (which starts at 120-150 m), OC
644 degradation in the water column and surface sediments should be depressed, so that
645 degradation might not be a significant cause for any reduction in f_M for the sediments.

646 In the Arabian Sea, the sediment trap material indicates the material is all marine
647 while the sediments show a small influence of non-marine material. The Arabian Sea site
648 was in an area of intense upwelling dominated by high export of diatomaceous material
649 (Wakeham et al., 2002), remote from fluvial inputs but potentially affected by aeolian
650 transport of pre-aged OC off the Arabian Peninsula and Horn of Africa during the windy
651 monsoon periods (Dahl et al., 2005). The AS trap was deployed within the OMZ where
652 organic matter degradation has reduced dissolved oxygen concentrations to $\sim 5 \mu\text{M}$
653 (Smith et al., 1998), but AS sediments were collected at 1400 m water depth where
654 bottom waters are oxygenated. Indeed within and below the OMZ, OC fluxes decreased
655 5-10 fold between the trap and surface sediments, even as %OC did not change as
656 dramatically (Lee et al., 2000 for OC; Wakeham et al., 2002 for AS lipid fluxes).
657 Comparative studies have shown conclusively that, among other things (e.g., intrinsic
658 reactivity of organic molecules and protection by macromolecular organic matrices and
659 mineral surfaces), oxygen availability is a key control on OC and lipid
660 degradation/preservation water columns and sediments (e.g., Hedges and Keil, 1995;

661 Gong and Hollander, 1997; Wakeham and Canuel, 2006; Burdige, 2007; Mollenhauer
662 and Eglinton, 2007). Enhanced degradation (diminished preservation) in the oxygenated
663 AS should be greater than in the anoxic Black Sea, and if marine OC is more labile than
664 terrigenous/relict OC, f_M in the AS POM and SOM would, as observed, be higher than in
665 the BS. Extensive production of petroleum reserves on the Arabian Peninsula and intense
666 tanker traffic in the Arabian Sea is an additional source of refractory and radiocarbon-
667 dead petrogenic OC to AS particulate matter and sediments.

668 The RS sediment results are consistent with previous studies suggesting that
669 marine material is the most important source of organic matter to the sediments (Arrigo et
670 al., 2002; Dunbar et al., 2003). The solutions that suggest a relatively large input of
671 vascular plant material seem unrealistic given these prior studies. The Ross Sea data set
672 is very limited and in fact does not include unambiguous lipids of either terrestrial or
673 relict origins with which to constrain the isotopic compositions of these endmembers.

674

675 **4 Conclusions**

676 This study examined the compound-specific ^{13}C and ^{14}C compositions of diverse
677 biomarker indicators of marine biomass, terrigenous vascular plant, and relict sources of
678 organic carbon in sediment traps and underlying surface sediments in the Black Sea, the
679 Arabian Sea and the Ross Sea. Using an isotopic mass balance approach, it was possible
680 to constrain relative inputs from these three sources, with marine biomass accounting for
681 66-100% of extractable lipids and organic carbon in Black Sea and Arabian Sea sediment
682 trap material. The remaining 3-8% derives from terrigenous and 4-16% from relict
683 sources. Sediments contained lower proportions of marine biomarkers (66-90%) and

684 consequentially higher proportions of terrigenous and relict carbon (3-17% and 7-13%,
685 respectively). These results suggest that although particulate organic carbon is
686 overwhelmingly marine in origin, there are significant proportions of pre-aged
687 terrigenous and relict OC present. Because these latter fractions become proportionally
688 more important in sediments, it is likely that they are better preserved than the marine
689 component, and/or they reach the sediments by lateral advection rather than only by the
690 vertical sinking that affects the upper ocean-derived marine POC. This approach
691 demonstrates the strengths, and limitations, of such a multi-parameter approach for
692 studying marine OC cycling and budgeting.

693

694 **Acknowledgements**

695 We thank Susumo Honjo and Steve Manganini for providing the Black Sea
696 sediment trap material, Rob Dunbar Ross Sea trap material, and Tim Eglinton, Nao
697 Ohkouchi and Jacqueline Grebmeier for providing the Ross Sea sediments. Michael
698 Peterson helped with sediment trap and sediment collections in the Arabian Sea. Tamara
699 Pease helped with initial analytical workup. NOSAMS personnel are thanked for
700 assistance in sample processing there for ^{13}C and ^{14}C analyses. Grants OCE-9310364 and
701 OCE-9911678 from the U.S. National Science Foundation (NSF), and the NSF
702 Cooperative Agreement for the Operation of a National Ocean Sciences Accelerator
703 Mass Spectrometry Facility (OCE-0753487 and OCE-123966) supported this research.
704 SGW acknowledges the Hanse Wissenschaftskolleg (Hanse Institute for Advanced
705 Studies), Delmenhorst, Germany, for a fellowship that supported writing of this
706 manuscript.

707

708

709 **References**

710 Aller, R. C.: Bioturbation and remineralization of sedimentary organic matter: effects of
711 redox oscillation, *Chem. Geol.*, 114, 331-345, 1994.

712 Anderson, J. B., Brake, C., and Myers, N.: Sedimentation on the Ross Sea continental
713 shelf, *Mar. Geol.*, 57, 295 333, 1984.

714 Andrews, J. T., Domack, E. W., Cunningham, W. L., Leventer, A., Licht, K. J., Jull, A. J.
715 T., DeMaster, D. J., and Jennings, A. E.: Problems and possible solutions
716 concerning radiocarbon dating of surface marine sediments, Ross Sea,
717 Antarctica, *Quaternary Res.*, 52, 206–216, 1999.

718 Arrigo, K. R., DiTullio, G. R., Dunbar, R. B., Lizotte, M. P., Robinson, D. R., Van
719 Woert, M., and Worthen, D. L.: Phytoplankton taxonomic variability and nutrient
720 utilization and primary production in the Ross Sea, *J. Geophys. Res.*, 105, 8827-
721 8846, 2000.

722 Arthur M. A. and Dean W. E.: Organic-matter production and preservation and evolution
723 of anoxia in the Holocene Black Sea, *Paleoceanogr.*, 13, 395–411, 1998.

724 Belt, S.T., Allard, W. G., Massé, Robert, J.-M., and Rowland, S.J.: Highly branched
725 isoprenoids (HBIs): Identification of the most common and abundant sedimentary
726 isomers. *Geochim. Cosmochim. Ac.* 64, 3829-3851, 2000.

727 Bentley, P. N.: Characteristics and distribution of wind blown sediment, western
728 McMurdo Sound, Antarctica, Thesis, Victoria Univ. Wellington, N.Z. 46 pp,
729 1979.

730 Berkman, P. A., and Forman, S. L.: Pre-bomb radiocarbon and the reservoir correction
731 for calcareous marine species in the Southern Ocean, *Geophys. Res. Lett.*, 23,
732 363–66, 1996.

733 Berner, R. A.: Burial of organic carbon and pyrite sulfur in the modern ocean – its
734 geochemical and environmental significance, *Am. J. Sci.*, 282, 451–473, 1982.

735 Blair, N. E., Leithold, E. L., Ford, S. T., Peeler, K. A., Holmes, J. C., and Perkey, D. W.:
736 The persistence of memory: the fate of ancient sedimentary organic carbon in a
737 modern sedimentary system, *Geochim. Cosmochim. Ac.*, 67, 63– 73, 2003.

738 Burdige, D. J.: Burial of terrestrial organic matter in marine sediments: A re-assessment,
739 *Global Biogeochem. Cycles*, 19, GB4011, doi:10.1029/2004GB002368, 2001.

740 Burdige, D. J.: Preservation of organic matter in marine sediments: controls, mechanisms,
741 and an imbalance in sediment organic carbon budgets? *Chem. Rev.*, 107, 467–
742 485, 2007.

743 Burkins, M. B., Virginia, R. A., Chamberlain, R. A., and Wall D. H.: The origin of soil
744 organic matter in Taylor Valley, Antarctica, *Antarct. Ecol.*, 81, 2377-2391, 2000.

745 Chikaraishi, Y., Naraoka, H., and Poulson, S. R.: Hydrogen and carbon isotopic
746 fractionations of lipid biosynthesis amount terrestrial (C3, C4, and CAM) and
747 aquatic plants, *Phytochem.*, 65, 1369–1381, 2004.

748 Collister, J. W., Rieley, G., Stern, B., Eglinton, G., and Fry, B.: Compound-specific ^{13}C
749 analyses of leaf lipids from plants with differing carbon dioxide metabolisms,
750 *Org. Geochem.*, 21, 619-627, 1994.

751 Conte, M. H. and Weber, J. C.: Plant biomarkers in aerosols record isotopic
752 discrimination of terrestrial photosynthesis, *Nature*, 417, 639–641, 2002.

753 Cowie, G. L., and Hedges, J. I.: Biochemical indicators of diagenetic alteration in natural
754 organic mixtures, *Nature*, 369, 304-307, 1994.

755 Dahl, K. A., Oppo, D. W., Eglinton, T. I., Hughen, K. A., Curry W. B., Sirocko, F.:
756 Terrigenous plant wax inputs to the Arabian Sea: Implications for the
757 reconstruction of winds associated with the Indian Monsoon, *Geochim.
758 Cosmochim. Ac.*, 10, 2547–2558, 2005.

759 Dehairs, F., Kopczynska, E., Nielsen, P., Lancelot, C., Bakker, D. C. E., Koeve, W., and
760 Goyens, L.: $\delta^{13}\text{C}$ of Southern Ocean suspended organic matter during spring and
761 early summer: Regional and temporal variability, *Deep-Sea Res., Part II*, 44, 129–
762 142, doi:10.1016/S0967- 0645(96)00073-2, 1997.

763 DeMaster, D. J., Ragueneau, O., and Nittrouer, C. A.: Preservation efficiencies and
764 accumulation rates for biogenic silica and organic C, N, and P in high-latitude
765 sediments: the Ross Sea, *J. Geophys. Res.*, 101, 18501–18518, 1996.

766 Domack, E. W., Jull, A. J. T., Anderson, J. B., Linick, T. W., and Williams, C. R.:
767 Application of tandem accelerator mass-spectrometer dating to Late-Pleistocene–
768 Holocene sediments of the East Antarctic continental shelf, *Quaternary Res.*, 31,
769 277–287, 1989.

770 Drenzek, N. J., Montluçon, D. B., Yunker, M. B., Macdonald, R. W., and Eglinton, T. I.:
771 Constraints on the origin of sedimentary organic carbon in the Beaufort Sea from
772 coupled molecular ^{14}C and ^{13}C measurements, *Mar. Chem.*, 103, 146–162, doi:
773 10.1016/j.marchem.2006.06.017, 2007.

774 Drenzek, N. J., Hughen, K. A., Montluçon, D. B., Southon, J. R., dos Santos, G. M.,

775 Druffel, E. R. M., Giosan, L., and Eglinton, T. I.: A new look at old carbon in

776 active margin sediments, *Geology*, 37, 239–242, doi: 10.1130/G25351A.1, 2009.

777 Druffel, E. R. M., Bauer, J. E., Williams, P. M., Griffin, S., and Wolgast, D.: Seasonal

778 variability of particulate organic radiocarbon in the northeast Pacific Ocean, *J.*

779 *Geophys. Res.*, 101:20,543-20,552, 1996.

780 Dunbar, R. B., Anderson, J. B., Domack, E. W.: Oceanographic influences on

781 sedimentation along the Antarctic Continental Shelf, *Antarctic Res. Ser.*,

782 American Geophysical Union, 45, 291–312, 1985.

783 Dunbar, R. B., Leventer, A. R., and Stockton, W. L.: Biogenic sedimentation in

784 McMurdo Sound, Antarctica, *Mar. Geol.*, 85, 155-179, 1989.

785 Dunbar, R. B., Arrigo, K. R., Lutz, M., DiTullio, G. R., Leventer, A. R., Lizotte, M. P.,

786 Van Woert, M. P., and Robinson, D. H.: Non-Redfield production and export of

787 marine organic matter: a recurrent part of the annual cycle in the Ross Sea, in:

788 *Biogeochemistry of the Ross Sea*, Antarctic Research Series Monograph, 78,,

789 edited by: DiTullo, G.R., and Dunbar, R.B., American Geophysical Union, 179-

790 195, 2003.

791 Eglinton, T. I., Aliwhare, L. I., Bauer, J. E., Druffel, E. R. M. and McNichol, A. P.: Gas

792 chromatographic isolation of individual compounds from complex matrices for

793 radiocarbon dating, *Anal. Chem.*, 68, 904-912, 1996.

794 Eglinton, T. I., Benitez-Nelson, B. C., Pearson, A., McNichol, A. P., Bauer, J. E., and

795 Druffel, E. R. M.: Variability in radiocarbon ages of individual organic

796 compounds from marine sediments, *Science*, 277, 796–799, 1997.

797 Eglinton, T. I., Eglinton, G., Dupont, L., Sholkovitz, E. R., Montlucon, D. and Reddy, C.
798 M.: Composition, age, and provenance of organic matter in NW African dust over
799 the Atlantic Ocean, *Geochem. Geophys. Geosys.*, 3, 1-27,
800 doi:10.1029/2001gc000269, 2002.

801 Feng, X., Benitez-Nelson, B. C., Montluçon, D. B., Prahl, F. G., McNichol, A. P., Xu, L.,
802 Repeta, D. J., and Eglinton, T. I.: ^{14}C and ^{13}C characteristics of higher plant
803 biomarkers in Washington margin surface sediments, *Geochim. Cosmochim. Ac.*,
804 105, 14–30, 2013.

805 Freeman K. H., Hayes J. M., Trendel J.-M., and Albrecht P.: Evidence from carbon
806 isotope measurements for diverse origins of sedimentary hydrocarbons, *Nature*,
807 343, 254-256, 1990.

808 Freeman K. H.: Isotopic biogeochemistry of marine organic carbon, in: *Stable Isotope*
809 *Geochemistry, Reviews in Mineralogy and Geochemistry*, vol. 43, edited by
810 Valley, J. W. and Cole, D. R., 579-605, 2001.

811 Fry, B., and Sherr, E. B.: $\delta^{13}\text{C}$ Measurements as indicators of carbon flow in marine and
812 freshwater ecosystems, *Mar. Sci.*, 27, 13–47 1984.

813 Gagosian, R. B., and Peltzer, E. T.: The importance of atmospheric input of terrestrial
814 organic material to deep sea sediments, *Org. Geochem.* 10, 661-669, 1986.

815 Gong, C., and Hollander, D. J.: Differential contribution of bacteria to sedimentary
816 organic matter in oxic and anoxic environments, Santa Monica Basin, California,
817 *Org. Geochem.*, 26, 545-563, 1997.

818 D. R., Martin, W. R., and Eglinton, T. I.: The radiocarbon age of organic carbon in
819 marine surface sediments, *Geochim. Cosmochim. Ac.*, 74, 6788–6800, 2010.

820 Gibson, J. A. E., Trull, T., Nichols, P. D., Summons, R. E., and McMinn, A.:
821 Sedimentation of C-13-rich organic matter from Antarctic sea-ice algae: A
822 potential indicator of past sea-ice extent, *Geology*, 27, 331-334, 1999.

823 Gleitz, M., Kukert, H., Riebesell, U., and Dieckmann, G. S.: Carbon acquisition and
824 growth of Antarctic sea ice diatoms in closed bottle incubations, *Mar. Ecol. Prog. Ser.*, 135, 169-177, 1996.

825 Haake, B., Rixen, T., Reemtsma, T., Ramaswamy, V., and Ittekkot, V.: Processes
827 determining seasonal variability and interannual variability of settling particle
828 fluxes to the deep Arabian Sea, in: *Particle Flux in the Ocean*, SCOPE vol. 57,
829 edited by Ittekkot, V., Schaefer, P., Honjo, S., and Depetris, P. J., 251-270, Wiley,
830 New York, 1996.

831 Gordon, J. E., and Harkness, D. D.: Magnitude and geographic variation of the
832 radiocarbon content in Antarctic marine life: implications for reservoir corrections
833 in radiocarbon dating, *Quaternary Sci. Rev.*, 11, 697-708, 1992.

834 Hall, B., Henderson, G., Baroni, C., and Kellogg, T.: Constant Holocene Southern Ocean
835 ^{14}C reservoir ages and ice-shelf flow rates. *Earth Planet. Sci. Lett.*, 296, 115-123,
836 2010.

837 Harris, P.T., O'Brien, P.E., Sedwick, P., and Truswell, E.M.: Late Quaternary history of
838 sedimentation on the Mac. Robertson Shelf, East Antarctica: problems with ^{14}C -
839 dating of marine sediment cores, *Proc. Roy. Soc. Tasmania*, 130, 47-53 1996.

840 Hayes, J.N.: Fractionation of the isotopes of carbon and hydrogen in biosynthetic
841 processes, in: *Stable Isotope Geochemistry, Reviews in Mineralogy and*

842 Geochemistry, vol. 43, edited by: Valley, J.W. and Cole, D.R., 225-278,
843 Mineralogical society of America, Washington DC, 2001.

844 Hay, B. J., Honjo, S., Kempe, S., Ittekkot, V., Degens, E. T., Konuk, T., and Izdar, E.:
845 Interannual variability in particle flux in the southwestern Black Sea, Deep-Sea
846 Res., 37, 911-928, 1990.

847 Hay, B. J., and Honjo, S.: Particle deposition in the present and Holocene Black Sea,
848 Oceanogr., 2, 26-31, 1989.

849 Hay B. J.: Particle flux in the western Black Sea in the present and over the last 5000
850 years: Temporal variability, sources, transport mechanisms. Ph.D. thesis,
851 WHOI-87-44. 201 pp .. MIT-WHOI Joint Program, 1987.

852 Hay, B. J., Arthur, M. A., Dean, W.: Sediment deposition in the Late Holocene abyssal
853 Black Sea with climatic and chronological implications, Deep-Sea Res., 38, Suppl
854 2, S1211-S1235, 1991.

855 Hedges, J. I., Hu, F. S., Devol, A. H., Hartnett, H. E., Tsamakis, E., and Keil, R. G.:
856 Sediment organic matter preservation; a test for selective degradation under oxic
857 conditions, Am. J. Sci., 299, 529-555; doi:10.2475/ajs.299.7-9.529, 1999.

858 Hedges, J. I., Baldock, J. A., Gelinas, Y., Lee, C., Peterson, M. L., and Wakeham, S. G.:
859 Non-selective preservation of organic matter in sinking marine particles, Nature,
860 409, 801-804, 2001.

861 Hedges J. I., and Keil R. G.: Sedimentary organic matter preservation: an assessment and
862 speculative synthesis, Mar. Chem., 49, 81-115, 1995.

863 Hedges, J. I., Keil, R. G., and Benner, R.: What happens to terrestrial organic matter in
864 the ocean? Org. Geochem., 27, 195-212, 1997.

865 Hedges, J. I., Eglinton, G., Hatcher, P. G., Kirchman, D. L., Arnosti, C., Derenne, S.,
866 Evershed, R. P., Kögel-Knabner, I., de Leeuw, J. W., Littke, R., Michaelis, W.
867 and Rullkötter, J.: The molecularly-uncharacterized component of nonliving
868 organic matter in natural environments, *Org. Geochem.*, 31, 945-958, 2000.

869 Honjo, S., Dymond, J., Prell, W., and Ittekkot, V.: Monsoon-controlled export fluxes to
870 the interior of the Arabian Sea, *Deep-Sea Res. II*, 46, 1859-1902, 1999.

871 Hwang, J., Druffel, E., and Komada, T.: Transport of organic carbon from the California
872 coast to the slope region: a study of $\Delta^{14}\text{C}$ and $\delta^{13}\text{C}$ signatures of organic
873 compound classes, *Global Biogeochem. Cycles*, 19, GB2018,
874 doi:10.1029/2004GB002422, 2005.

875 Hwang, J., Druffel, E. R. M., and Eglinton, T. I.: Widespread influence of resuspended
876 sediments on oceanic particulate organic carbon: Insights from radiocarbon and
877 aluminum contents in sinking particles, *Global Biogeochem. Cycles*, 24, GB4016,
878 doi:10.1029/2010GB003802, 2010.

879 Ingalls A. E. and Pearson A.: Ten years of compound-specific radiocarbon analysis,
880 *Oceanography*, 18, 18-31, 2005.

881 Jones, G. A. and Gagnon, A. R.: Radiocarbon chronology of Black Sea sediments, *Deep-*
882 *Sea Research*, 41, 531-557, 1994.

883 Kawamura, K., Ishimura, Y., and Yamazaki, K.: Four years' observations of terrestrial
884 lipid class compounds in marine aerosols from the western North Pacific, *Global*
885 *Biogeochem. Cycles*, 17, 1003, doi:10.1029/2001GB001810, 2003.

886 Key, R. M., Kozyr, A., Sabine, C. L., Lee, K., Wanninkhof, R., Bullister, J. L., Feely, R.
887 A., Millero, F. J., Mordy, C., and Peng, T.-H.: A global ocean carbon

888 climatology: Results from Global Data Analysis Project (GLODAP), Global
889 Biogeochem. Cy., 18, GB4031, doi:10.1029/2004GB002247, 2004.

890 Komada, T., Druffel, E., and Hwang, J.: Sedimentary rocks as sources of ancient organic
891 carbon to the ocean: an investigation through $\Delta^{14}\text{C}$ and $\delta^{13}\text{C}$ signatures of
892 compound classes, Global Biogeochem. Cycles, 19, GB2017,
893 doi:10.1029/2004GB002347, 2005.

894 Kusch, S., Rethemeyer, J., Schefuß, E., and Mollenhauer, G.: Controls on the age of
895 vascular plant biomarkers in Black Sea sediments, Geochim. Cosmochim. Ac.,
896 74, 7031-7047, 2010.

897 Lee, C., Murray, D. W., Barber, R. T., Buesseler, K. O., Dymond, J., Hedges, J. I.,
898 Honjo, S., Manganini, S.J., Marra, J., Moser, C., Peterson, M. L., Prell, W. L., and
899 Wakeham, S. G.: Particulate organic carbon fluxes: compilation of results from
900 the 1995 US JGOFS Arabian Sea Process Study, Deep-Sea Res. II, 45, 2489-
901 2501, 1998.

902 Lee, C., Wakeham, S. G., and Arnosti, C.: Particulate organic matter in the sea: the
903 composition conundrum, Ambio, 33, 565-575, 2004.

904 Levin, I., and Kromer, B.; Twenty years of atmospheric $^{14}\text{CO}_2$ observations at
905 Schauinsland, Radiocarbon, 39, 205-218, 1997.

906 Licht, K. J., Jennings, A. E., Andrews, J. T., and Williams, K. M.: Chronology of late
907 Wisconsin ice retreat from the western Ross Sea, Antarctica, Geol., 24, 223-226,
908 1996.

909 McNichol A. P., Osborne E. A., Gagnon A. R., Fry B., and Jones G. A.: TIC, TOC, DIC,
910 DOC, PIC, POC – unique aspects in the preparation of oceanographic samples for

911 ¹⁴C-AMS, Nucl. Instr. Meth. Phys. Res., Sect. B92, 162-165, 1994.

912 913 McNichol, A.P., and Aluwihare, L. I.: The power of radiocarbon in biogeochemical studies of the marine carbon cycle: Insights from studies of dissolved and

914 particulate organic carbon (DOC and POC), Chem. Rev. 107, 443-466, 2007.

915 916 Mollenhauer, G., Eglinton, T. I., Ohkouchi, N., Schneider, R. R., Müller, P. J., Grootes, P. M., and Rullkötter, J.: Asynchronous alkenone and foraminifera records from

917 the Benguela Upwelling System, Geochim. Cosmochim. Ac., 67, 2157-2171,

918 2003.

919 920 Mollenhauer, G., and Eglinton, T. I.: Diagenetic and sedimentological controls on the composition of organic matter preserved in California Borderland Basin

921 sediments, Limnol. Oceanogr., 52, 558-576, 2007.

922 923 Ohkouchi, N., Eglinton, T. I., Keigwin, L. D., and Hayes, J. M.: Spatial and temporal offsets between proxy records in a sediment drift, Science, 298, 1224-1227, 2002.

924 925 Ohkouchi, N., Eglinton, T. I., and Hayes, J. M.: Radiocarbon dating of individual fatty acids as a tool for refining Antarctic Margin sediment chronologies,

926 Radiocarbon, 45, 17-24, 2003.

927 928 Ohkouchi, N., and Eglinton, T. I.: Compound-specific radiocarbon dating of Ross Sea sediments: A prospect for constructing chronologies in high-latitude oceanic

929 sediments, Quart. Geochronol., 3, 235-243, 2008.

930 931 Ohkouchi, N., Xu, L., Reddy, C. M., Montluçon, D., and Eglinton, T. I.: Radiocarbon dating of alkenones from marine sediments, I. Isolation protocol, Radiocarbon,

932 47, 401-412, 2005.

933 Passier, H. F., Luther, G.W, III., and de Lange, G. J.: Early diagenesis and sulfur
934 speciation in sediments of the Oman Margin, northwestern Arabian Sea, Deep-
935 Sea Res., 44, 1361-1380, 1997.

936 Pearson A.: Biogeochemical applications of compound-specific radiocarbon analysis,
937 Ph.D. Thesis, Woods Hole Oceanographic Institution/Massachusetts Institute of
938 Technology, Woods Hole, MA, 248 pp, 2000.

939 Pearson, A.: Pathways of carbon assimilation and their impact on organic matter values
940 of $\delta^{13}\text{C}$, in: Handbook of Hydrocarbon and Lipid Microbiology: Microbial
941 interactions with hydrocarbons, oils, fats, and related hydrophobic substrates and
942 products, edited by: K. Timmis, 143-156, Springer-Verlag Berlin, DOI
943 10.1007/978-3-540-77587-4_9, 2010.

944 Pearson, A., and Eglinton, T. I.: The origin of *n*-alkanes in Santa Monica Basin surface
945 sediment: a model based on compound-specific $\Delta^{14}\text{C}$ and $\delta^{13}\text{C}$ data. Org.
946 Geochem. 31, 1103-1116, 2000.

947 Pearson A., McNichol A. P., Schneider R. J. and von Reden K. F.: Microscale AMS ^{14}C
948 measurement at NOSAMS, Radiocarbon, 40, 61-76, 1998.

949 Pearson A., McNichol A. P., Benetiz-Nelson B. C., Hayes J. M., and Eglinton T. I.:
950 Origins of lipid biomarkers in Santa Monica Basin surface sediment: A case study
951 using compound-specific $\Delta^{14}\text{C}$ analysis, Geochim. Cosmochim. Ac., 65, 3123-
952 3137, 2001.

953 Pearson A., Seewald J. S. and Eglinton T. I.: Bacterial incorporation of relict carbon in the
954 hydrothermal environment of Guaymas Basin, Geochim. Cosmochim. Ac., 69,
955 5477-5486, 2005.

956 Petsch, S. T., Eglinton, T. I., and Edwards, K. J.: ^{14}C -dead living biomass: Evidence for
957 microbial assimilation of ancient organic carbon during shale weathering,
958 *Science*, 292, 1127-1131, doi: 10.1126/science.1058332, 2001.

959 Petsch, S. T., Edwards, K. J., and Eglinton, T. I.: Abundance, distribution, and $\delta^{13}\text{C}$
960 analysis of microbial phospholipid-derived fatty acids in a black shale weathering
961 profile, *Org. Geochem.*, 34, 731-743, doi: 10.1016/S0146-6380(03)00040-8,
962 2003.

963 Prahl F. G., Muehlhausen L. A., and Lyle, M.: An organic geochemical assessment of
964 oceanographic conditions at MANOP Site C over the past 26,000 years,
965 *Paleoceanogr*, 4, 495-510, 1989.

966 Premuzic E. T., Benkovitz C. M., Gaffney J. S., and Walsh J. J.: The nature and
967 distribution of organic matter in the surface sediments of world oceans and seas,
968 *Org. Geochem.*, 4, 63-77, 1982.

969 Ramage C. S., Miller F. R., and Jeffries C.: Meteorological Atlas of the International
970 Indian Ocean Expedition: The Surface Climate of 1963, 1964, U.S. National
971 Science Foundation and India Meteorological Department, 1972.

972 Rau, G. H., Takahashi, T., Des Marias, D. J., and Sullivan, C. W.: Particulate organic
973 matter δC variations across the Drake Passage, *J. Geophys. Res.*, 96, 15,131-
974 15,135, doi:10.1029/91JC01253, 1991.

975 Rau, G. H., C. W. Sullivan, and L. I. Gordon (1991), $\delta^{13}\text{C}$ and $\delta^{15}\text{N}$ variations in Weddell
976 Sea particulate organic matter, *Mar. Chem.*, 35, 355-369, doi:10.1016/S0304-
977 4203(09)90028-7, 1991.

1001 Stuiver M., and Ostlund, H. G.: GEOSECS Indian Ocean and Mediterranean radiocarbon.

1002 Radiocarbon 25, 1–29, 1983.

1003 Stuiver, M., and Braziunas, T. F.: Modelling atmospheric ^{14}C influences and ^{14}C ages of

1004 marine samples to 10,000 BP, Radiocarbon, 35, 137– 189, 1993.

1005 Villinski, J. C., Dunbar, R. B., and Mucciarone, D. A.: Carbon 13/ Carbon 12 ratios of

1006 sedimentary organic matter from the Ross Sea, Antarctica: A record of

1007 phytoplankton bloom dynamics, J. Geophys. Res., 105(C6), 14,163–14,172,

1008 doi:10.1029/1999JC000309, 2000.

1009 Volkman J. R, Eglinton G., Corner E. D. S. and Forsberg T. E. V.: Long-chain alkenes

1010 and alkenones in the marine coccolithophorid *Emiliania huxleyi*. Phytochem., 19,

1011 2619-2622, 1980.

1012 Volkman, J.K.: Lipid markers for marine organic matter, in: The Handbook of

1013 Environmental Chemistry, edited by: Hutzinger, O.; Vol 2: Reactions and

1014 processes, Part N, Marine organic matter: Biomarkers, isotopes and DNA, edited

1015 by Volkman, J.K. Springer, Berlin, 27-70, 2006.

1016 von Reden K. F., Schneider R. F., McNichol A. P., and Pearson A.: ^{14}C -AMS

1017 measurements of < 100 μg samples with a high-current system, Radiocarbon 40,

1018 247-253, 1998.

1019 Wakeham, S. G.: Organic matter from a sediment trap experiment in the equatorial

1020 Atlantic: wax esters, steryl esters, triacylglycerols, and alkyldiacylglycerols,

1021 Geochim. Cosmochim. Ac. 46, 2239-2257, 1982.

1022 Wakeham, S. G.: Aliphatic and polycyclic aromatic hydrocarbons in Black Sea

1023 sediments, Mar. Chem., 53, 187-205, 1996.

1024 Wakeham, S. G., and Canuel, E. A.: Degradation and preservation of organic matter in
1025 marine sediments, in: The Handbook of Environmental Chemistry, Vol. 2,
1026 Reactions and Processes, edited by: Hutzinger, O.; Vol. 2. Marine Organic
1027 Matter: Biomarkers, Isotopes and DNA, edited by: Volkman, J. K., Springer-
1028 Verlag, Berlin, 295-321, 2006.

1029 Wakeham, S. G., Beier, J. A., and Clifford, C. H.: Organic matter sources in the Black
1030 Sea as inferred from hydrocarbon distributions, in: Black Sea Oceanography,
1031 edited by: Izdar, E., and Murray, J. W., Kluwer, 319-341, 1991.

1032 Wakeham, S. G., Lee, C., Hedges, J. I., Hernes, P. J., and Peterson, M. L.: Molecular
1033 indicators of diagenetic status in marine organic matter, *Geochim. Cosmochim. Ac.*, 61, 5363-5369, 1997.

1035 Wakeham, S. G., Peterson, M. L., Hedges J. I., and Lee, C.: Lipid biomarker fluxes in the
1036 Arabian Sea: with a comparison to the Equatorial Pacific Ocean, *Deep-Sea Res.*
1037 II., 49, 2265-2301, 2002.

1038 Wakeham, S. G., McNichol, A. P., Kostka, J., and Pease, T. K.: Natural abundance
1039 radiocarbon as a tracer of assimilation of petroleum carbon by bacteria in salt
1040 marsh sediments, *Geochim. Cosmochim. Ac.*, 70, 1761-1771, 2006.

1041 Wang, X.-C., Druffel, E. R. M., Griffin, S., Lee, C., and Kashgarian, M.: Radiocarbon
1042 studies of organic compound classes in plankton and sediment of the northeastern
1043 Pacific Ocean, *Geochim. Cosmochim. Ac.*, 62, 1365-1378, 1998.

1044 Wang, X.-C., and Druffel, E. R. M.: Radiocarbon and stable carbon isotope compositions
1045 of organic compound classes in sediments from the NE Pacific and Southern
1046 Oceans, *Mar. Chem.*, 73, 65-81, 2001.

1047 Yunker, M. B., Macdonald, R. W., Cretney, W. J., Fowler, B. R., and McLaughlin, F. A.:
1048 Alkane, terpene and polycyclic aromatic hydrocarbon geochemistry of the
1049 Mackenzie River and Mackenzie shelf: Riverine contributions to Beaufort Sea
1050 coastal sediment, *Geochim. Cosmochim. Ac.*, 57, 3041-3061, 1993.
1051 Yunker, M. B., Backus, S. M., Pannatier, E. G., Jeffries, D. S., and Macdonald, R. W.:
1052 Sources and significance of alkane and PAH hydrocarbons in Canadian arctic
1053 rivers, *Estuar. Coast. Shelf S.*, 55, 1-31, 2002.
1054 Zafiriou, O. C., Gagosian, R. B., Peltzer, E. T., and Alford, J. B.: Air-to-sea fluxes of
1055 lipids at Enewetak Atoll, *J. Geophys. Res.*, 90, 2409-2423, 1985.
1056 Zonneveld, K. A. F., Versteegh, G. J. M., Kasten, S., Eglinton, T., Emeis, K.-C., Huguet,
1057 C., Koch, B., de Lange, G. J., de Leeuw, J. W., Middelburg, J. J., Mollenhauer,
1058 G., Prahl, F., Rethemeyer, J., and Wakeham, S.: Selective preservation of organic
1059 matter in marine environments; processes and impact on the fossil record,
1060 *Biogeosci.*, 7, 483-511, 2010.
1061
1062
1063

Table 1. Stable carbon and radiocarbon isotope data for Black Sea POM and SOM.

Black Sea Trap						
	source	ID #	$\delta^{13}\text{C}$ (‰)	$\Delta^{14}\text{C}$ (‰)	<i>fm</i>	Age
OC		OS-32870	-22.9	21 ± 2	1.026 ± 0.003	>Mod
SLE		OS-38316	-27.2	-96 ± 16	0.909 ± 0.016	770 ± 140
14:0 FA	M	OS-38328	-25.6	132 ± 13	1.064 ± 0.014	>Mod
b-15:0 FA	M	OS-38321	-25.3	90 ± 9	1.029 ± 0.011	>Mod
16:1 FA	M	OS-38327	-25.4	81 ± 11	1.025 ± 0.011	>Mod
16:0 FA	M	OS-38333	-24.3	146 ± 9	1.086 ± 0.011	>Mod
18:1 FA	M	OS-38318	-23.2	288 ± 11	1.228 ± 0.008	>Mod
18:0 FA	M	OS-38320	-23.9	77 ± 11	1.028 ± 0.011	>Mod
24+26+28 FA	T	OS-38331	-27.0	1 ± 16	0.967 ± 0.014	265 ± 110
alkenones	M	OS-39539	-26.6	87 ± 14	1.099 ± 0.014	>Mod
24+26+28 HC	R	OS-39911	-29.3	-677 ± 10	0.325 ± 0.009	9030 ± 210
27+29 HC	T	OS-39908	-30.0	-181 ± 14	0.825 ± 0.010	1550 ± 100
27 Δ^5 sterol	M	OS-53936	-26.4	79 ± 11	1.046 ± 0.011	>Mod.
28 $\Delta^{5,22}$ sterol	M	OS-53934	-26.1	65 ± 9	1.034 ± 0.009	>Mod.
30 Δ^{22} sterol	M	OS-53957	-25.7	69 ± 15	1.040 ± 0.015	>Mod.
24+26+28 ROH	T	OS-53956	-30.1	-44 ± 12	0.925 ± 0.012	625 ± 110
Black Sea Sediment						
OC		OS-32871	-25.3	-199 ± 6	0.806 ± 0.004	1740 ± 35
SLE		OS-38309	-27.9	-150 ± 15	0.856 ± 0.008	1250 ± 80
14:0 FA	M	OS-38630	-28.6	18 ± 15	0.957 ± 0.016	350 ± 130
b-15:0 FA	M	OS-38632	-30.5	-27 ± 14	0.919 ± 0.019	680 ± 170
16:1 FA	M	OS-38628	-31.9	75 ± 14	1.019 ± 0.013	>Mod
16:0 FA	M	OS-38627	-29.1	214 ± 18	1.151 ± 0.018	>Mod
b-17:0 FA	M	OS-38642	-30.5	57 ± 20	1.006 ± 0.020	>Mod
18:1 FA	M	OS-38637	-27.0	-24 ± 20	0.999 ± 0.020	5 ± 100
18:0 FA	M	OS-38636	-29.5	374 ± 27	1.310 ± 0.023	>Mod
22:0 FA	M	OS-38639	-28.9	-46 ± 26	0.919 ± 0.027	680 ± 230
24:0 FA	M	OS-38640	-29.2	-34 ± 26	0.934 ± 0.024	550 ± 220
26:0 FA	T	OS-38641	-30.5	-223 ± 31	0.754 ± 0.021	2270 ± 230
alkenones	M	OS-39536	-28.6	45 ± 13	1.069 ± 0.013	>Mod
24+26+28 HC	R	OS-39909	-29.2	-609 ± 11	0.393 ± 0.007	7500 ± 150
27 HC	T	OS-39907	-30.0	-231 ± 8	0.774 ± 0.011	2060 ± 110
29 HC	T	OS-39906	-31.0	-125 ± 8	0.880 ± 0.008	1020 ± 75
27 Δ^5 sterol	M	OS-53948	-27.0	-33 ± 12	0.937 ± 0.012	520 ± 100
30 Δ^{22} sterol	M	OS-53943	-26.0	-15 ± 9	0.942 ± 0.011	475 ± 95
24 ROH	T	OS-53951	-29.7	-176 ± 8	0.796 ± 0.011	1840 ± 110
26 ROH	T	OS-53958	-31.2	-100 ± 16	0.871 ± 0.018	1100 ± 160

M = marine; T = terrigenous; R = relict

FA = fatty acid; ROH = alcohol; HC = alkane

Table 2. Stable carbon and radiocarbon isotope data for Arabian Sea POM and SOM.

Arabian Sea Trap						
	source	ID #	$\delta^{13}\text{C}$ (‰)	$\Delta^{14}\text{C}$ (‰)	fm	Age
OC		OS- 32868	-22.4	14 ± 13	1.020 ± 0.013	>Mod
SLE		OS- 38314	-24.7	66 ± 14	1.073 ± 0.014	>Mod
14:0 FA	M	OS- 37311	-25.7	178 ± 17	1.107 ± 0.017	>Mod
b-15:0 FA	M	OS- 37314	-23.2	56 ± 13	0.997 ± 0.014	25 ± 110
16:1 FA	M	OS- 37304	-24.0	55 ± 21	0.999 ± 0.014	5 ± 100
16:0 FA	M	OS- 37298	-23.8	97 ± 14	1.039 ± 0.013	>Mod
18:1 FA	M	OS- 37297	-23.1	38 ± 21	0.990 ± 0.013	80 ± 100
18:0 FA	M	OS- 37302	-23.8	111 ± 15	1.060 ± 0.015	>Mod
22:0 FA	M	OS- 37305	-23.8	51 ± 14	1.012 ± 0.014	>Mod
24:0 FA	M	OS- 37313	-24.7	69 ± 14	1.033 ± 0.013	>Mod
26:0 FA	M	OS- 37315	-25.2	80 ± 16	1.047 ± 0.016	>Mod
alkenones	M	OS-39910	-23.9	-6 ± 9	1.000 ± 0.011	>Mod
24+26+28 HC	R	OS-55323	-28.5	-731 ± 14	0.270 ± 0.013	10500 ± 390
HBI HC	M	OS-55248	-24.5	-514 ± 10	0.488 ± 0.010	5750 ± 160
27+29 HC	T	OS-55325	-28.4	-320 ± 24	0.684 ± 0.024	3050 ± 280
27 Δ^5 sterol	M	OS-56344	-16.7	-32 ± 12	0.939 ± 0.012	505 ± 100
28 $\Delta^{5,22}$ sterol	M	OS-56348	-27.1	-86 ± 13	0.888 ± 0.013	955 ± 120
16 ROH	M	OS-56347	-22.5	-91 ± 12	0.861 ± 0.012	1200 ± 110
Arabian Sea Sediment						
OC		OS- 32869	-20.8	-138 ± 2	0.867 ± 0.003	1140 ± 30
LE		OS- 38322	-25.0	-173 ± 11	0.833 ± 0.011	1470 ± 100
14:0 FA	M	OS- 38332	-26.6	-10 ± 13	0.931 ± 0.013	575 ± 110
b-15:0 FA	M	OS- 38324	-24.5	-70 ± 11	0.878 ± 0.011	1040 ± 100
16:1 FA	M	OS- 38313	-26.0	-112 ± 7	0.842 ± 0.007	1380 ± 65
16:0 FA	M	OS- 38329	-25.0	104 ± 12	1.046 ± 0.012	>Mod
18:1 FA	M	OS- 38334	-24.8	-171 ± 13	0.791 ± 0.013	1880 ± 140
18:0 FA	M	OS- 38325	-24.7	190 ± 10	1.135 ± 0.010	>Mod
22:0 FA	M	OS- 38326	-26.8	103 ± 12	0.864 ± 0.012	1180 ± 110
24:0 FA	M	OS- 38317	-25.4	-91 ± 7	0.879 ± 0.006	1040 ± 55
26:0 FA	M	OS- 38319	-24.7	-116 ± 7	0.858 ± 0.007	1230 ± 70
alkenones	M	OS- 39902	-24.1	-202 ± 7	0.803 ± 0.003	1760 ± 65
24+26+28 HC	R	OS-55329	-27.6	-805 ± 9	0.197 ± 0.008	13050 ± 340
HBI HC	M	OS-56341	-18.2	-256 ± 8	0.748 ± 0.008	2330 ± 85
15+16+17+18 HC	R	OS-55251	-29.4	-887 ± 5	0.114 ± 0.004	17500 ± 250
27+29 HC	T	OS-55318	-27.7	-430 ± 11	0.573 ± 0.011	4470 ± 160
27 Δ^5 sterol	M	OS-56349	-24.0	-152 ± 13	0.822 ± 0.013	1570 ± 130
16 ROH	M	OS-56351	-23.3	-99 ± 13	0.853 ± 0.012	1270 ± 110
26+28+30 ROH	T	OS-56350	-24.1	-113 ± 14	0.861 ± 0.012	1200 ± 110

M = marine; T = terrigenous; R = relict

FA = fatty acid; ROH = alcohol; HC = alkane

Table 3. Stable carbon and radiocarbon isotope data for Ross Sea POM and SOM.

Ross Sea Trap						
	source	ID #	$\delta^{13}\text{C}$ (‰)	$\Delta^{14}\text{C}$ (‰)	<i>fm</i>	Age
OC		OS-32872	-28.0	-208 ± 6	0.797 ± 0.004	1820 ± 40
SLE		OS-38330	-32.7	-154 ± 15	0.852 ± 0.015	1290 ± 140
14:0 FA	M	OS-38626	-34.9	-115 ± 14	0.831 ± 0.012	1490 ± 110
16:0 FA	M	OS-38624	-31.7	-100 ± 10	0.853 ± 0.010	1270 ± 95
18:0 FA	M	OS-39272	-35.3	-105 ± 15	0.854 ± 0.015	1270 ± 140
22:0+24:0 FA	M	OS-38635	-31.8	-175 ± 19	0.796 ± 0.019	1830 ± 190
27 Δ^5 sterol	M	OS-50105	-32.0	-216 ± 7	0.761 ± 0.007	2190 ± 75
28 $\Delta^{5,22}$ sterol	M	OS-50107	-35.4	-180 ± 8	0.796 ± 0.007	1830 ± 70
14+16 ROH	M	OS-50100	-31.8	-191 ± 9	0.764 ± 0.008	2160 ± 80
Ross Sea Sediment						
OC		OS-32873	-27.9	-355 ± 3	0.649 ± 0.003	3480 ± 35
SLE		OS-38323	-30.0	-211 ± 18	0.795 ± 0.018	1850 ± 180
14:0 FA	M	OS-38633	-36.6	-83 ± 5	0.862 ± 0.015	1190 ± 140
br-15:0 FA	M	OS-38625	-32.3	-128 ± 12	0.824 ± 0.012	1560 ± 120
16:0 FA	M	OS-39266	-32.5	430 ± 11	1.439 ± 0.011	>Mod
18:0 FA	M	OS-38644	-31.0	189 ± 29	1.196 ± 0.029	>Mod
24:0 FA	M	OS-38634	-33.5	-208 ± 22	0.765 ± 0.023	2150 ± 240
26:0 FA	M	OS-38645	-30.3	-302 ± 27	0.677 ± 0.029	3130 ± 340
27 Δ^5 sterol	M	OS-50108	-33.0	-178 ± 10	0.798 ± 0.010	1810 ± 95
28 $\Delta^{5,22}$ sterol	M	OS-50106	-34.3	-202 ± 8	0.775 ± 0.007	2050 ± 70

FA = fatty acid; ROH = alcohol

1073

1074 Table 4. Abundance weighted mean table carbon and radiocarbon isotope values for
 1075 compositing marine, terrigenous, and relict biomarkers.

1076

	$\delta^{13}\text{C}$ (‰) \pm s.d.	$\Delta^{14}\text{C}$ (‰) \pm s.d.	$f_m \pm$ s.d.	Age \pm s.d.	n
BS trap					
marine	-25.3 \pm 1.1	78 \pm 9	1.110 \pm 0.066	>Mod	7
terrigenous	-28.7 \pm 1.6	-75 \pm 94	0.930 \pm 0.043	580 \pm 360	3
relict	-29.1	-677 \pm 9	0.325 \pm 0.009	9030 \pm 220	1
BS sediment					
marine	-28.8 \pm 1.8	-30 \pm 10	0.970 \pm 0.023	240 \pm 56	6
terrigenous	-30.5 \pm 0.7	-171 \pm 58	0.833 \pm 0.066	1470 \pm 615	5
relict	-29.2	-609 \pm 8	0.393 \pm 0.007	7500 \pm 150	1
AS trap					
marine	-23.5 \pm 2.5	64 \pm 20	1.071 \pm .019	>Mod	7
terrigenous	-26.8 \pm 2.3	-320 \pm 24	0.684 \pm 0.024	3050 \pm 280	2,1
relict	-28.5	-731 \pm 13	0.270 \pm 0.013	10140 \pm 360	1
AS sediment					
marine	-24.5 \pm 2.1	-63 \pm 110	0.941 \pm 0.110	490 \pm 1440	8
terrigenous	-27.7	-430 \pm 13	0.573 \pm 0.011	4470 \pm 150	1
relict	-28.5 \pm 1.2	-846 \pm 58	0.114 \pm 0.004	17440 \pm 270	1
RS trap					
marine	-33.3 \pm 1.8	-155 \pm 47	0.850 \pm .045	1310 \pm 420	7
terrigenous	nd*	nd*	nd*	nd*	nd*
relict	nd*	nd*	nd*	nd*	nd*
RS sediment					
marine	-33.2 \pm 1.9	-105 \pm 31	0.900 \pm 0.030	850 \pm 270	6
terrigenous	-31.8 \pm 2.8	-255 \pm 66	0.750 \pm 0.056	2310 \pm 560	2
relict	nd*	nd*	nd*	nd*	nd*

nd* not determined

1077

1078

1079

1080 Table 5. Isotopic values used in mass balance calculations. The values of f_M , f_T , and f_R
 1081 are those values calculated assuming that the actual value of $\Delta^{14}\text{C}_{\text{added}}$ is that measured on
 1082 the compounds defined as relict.

Sample	$\Delta^{14}\text{C}_{\text{bulk}} (\text{\textperthousand})$	$\Delta^{14}\text{C}_M (\text{\textperthousand})$	$\Delta^{14}\text{C}_T (\text{\textperthousand})$	$\Delta^{14}\text{C}_{\text{add}} (\text{\textperthousand})$	f_M	f_T	f_R
BS trap	-100	80	-75	-677	0.76	0.08	0.15
BS sed	-150	-30	-171	-609	0.79	0.1	0.11
AS trap	64	64	-320	-731	1	0	0
AS sed	-173	-63	-430	-846	0.86	0.04	0.1
RS sed	-210	-105	-255	--	--	--	--

1083

Figure Captions

Figure 1. Sampling locations in the Black Sea, Arabian Sea and Ross Sea.

Figure 2. Scheme of extraction, isolation and analysis of biomarkers.

Figure 3. (a) Organic carbon (%OC) and (b) C/N(a) for bulk trap and sediments.

Figure 4. (a) The $\delta^{13}\text{C}$ and (b) $\Delta^{14}\text{C}$ values of bulk organic carbon (OC) and (c) $\delta^{13}\text{C}$ and (d) $\Delta^{14}\text{C}$ values solvent extractable lipids (SLE) for trap POM and sediments.

Figure 5. Histograms of relative abundances of (a) fatty acids, (b) hydrocarbons, and (c) sterols/alcohols POM and SOM from the Black Sea. Carbon numbers are given for fatty acids, alkanes, and alcohols; sterol abbreviations are $27\text{D}5,22 = 27\Delta^{5,22}$, etc.

Figure 6. Histograms of relative abundances of (a) fatty acids, (b) hydrocarbons, and (c) sterols/alcohols in POM and SOM from the Arabian Sea. Carbon numbers are given for fatty acids, alkanes, and alcohols; sterol abbreviations are $27\text{D}5,22 = 27\Delta^{5,22}$, etc.

Figure 7. Histograms of relative abundances of (a) fatty acids, (b) hydrocarbons, and (c) sterols/alcohols in POM and SOM from the Ross Sea. Carbon numbers are given for fatty acids, alkanes, and alcohols; sterol abbreviations are $27\text{D}5,22 = 27\Delta^{5,22}$, etc.

Figure 8. The (a) $\delta^{13}\text{C}$ and (b) $\Delta^{14}\text{C}$ values of bulk POC and SOC and individual biomarkers for trap and sediments from the Black Sea (see also Table 1). Filled symbols are trap biomarkers; open symbols are sediment biomarkers. All values have been corrected for procedural blanks and any derivative carbon, as needed. Dashed lines are pre-bomb (lower) and post-bomb (upper) mixed-layer $\Delta^{14}\text{C}_{\text{DIC}}$.

Figure 9. The (a) $\delta^{13}\text{C}$ and (b) $\Delta^{14}\text{C}$ values of bulk POC and SOC and individual biomarkers for trap and sediments from the Arabian Sea (see also Table 2). Filled symbols are trap biomarkers; open symbols are sediment biomarkers. All values have been corrected for procedural blanks and any derivative carbon, as needed. Dashed lines are pre-bomb (lower) and post-bomb (upper) mixed-layer $\Delta^{14}\text{C}_{\text{DIC}}$.

Figure 10. The (a) $\delta^{13}\text{C}$ and (b) $\Delta^{14}\text{C}$ values of bulk POC and SOC and individual biomarkers for trap and sediments from the Ross Sea (see also Table 3). Filled symbols are trap biomarkers; open symbols are sediment biomarkers. All values have been corrected for procedural blanks and any derivative carbon, as needed. Dashed lines are pre-bomb (lower) and post-bomb (upper) mixed-layer $\Delta^{14}\text{C}_{\text{DIC}}$.

Figure 11. Concentration weighted average $\delta^{13}\text{C}$ and $\Delta^{14}\text{C}$ values of marine (M), terrigenous (T) and relict (R) lipids in (a) Black Sea, (b) Arabian Sea, and (c) Ross Sea traps and sediments.

Figure 12. Relative amounts of marine (M, blue solid line), terrestrial (T, red dashed line) and relict (R, black small-dashed line) carbon as a function of $\Delta^{14}\text{C}_{\text{add}}$ in Black Sea and Arabian Sea trap material (a and c, respectively) and in Black Sea, Arabian Sea and Ross Sea sediments (b, d, and e, respectively). Only real solutions are depicted. The solid black line indicates the solution when $\Delta^{14}\text{C}_{\text{added}}$ is equal to the value measured on compounds defined as relict. There are not enough data to construct a graph for the Ross Sea sediment trap.

Figure 1

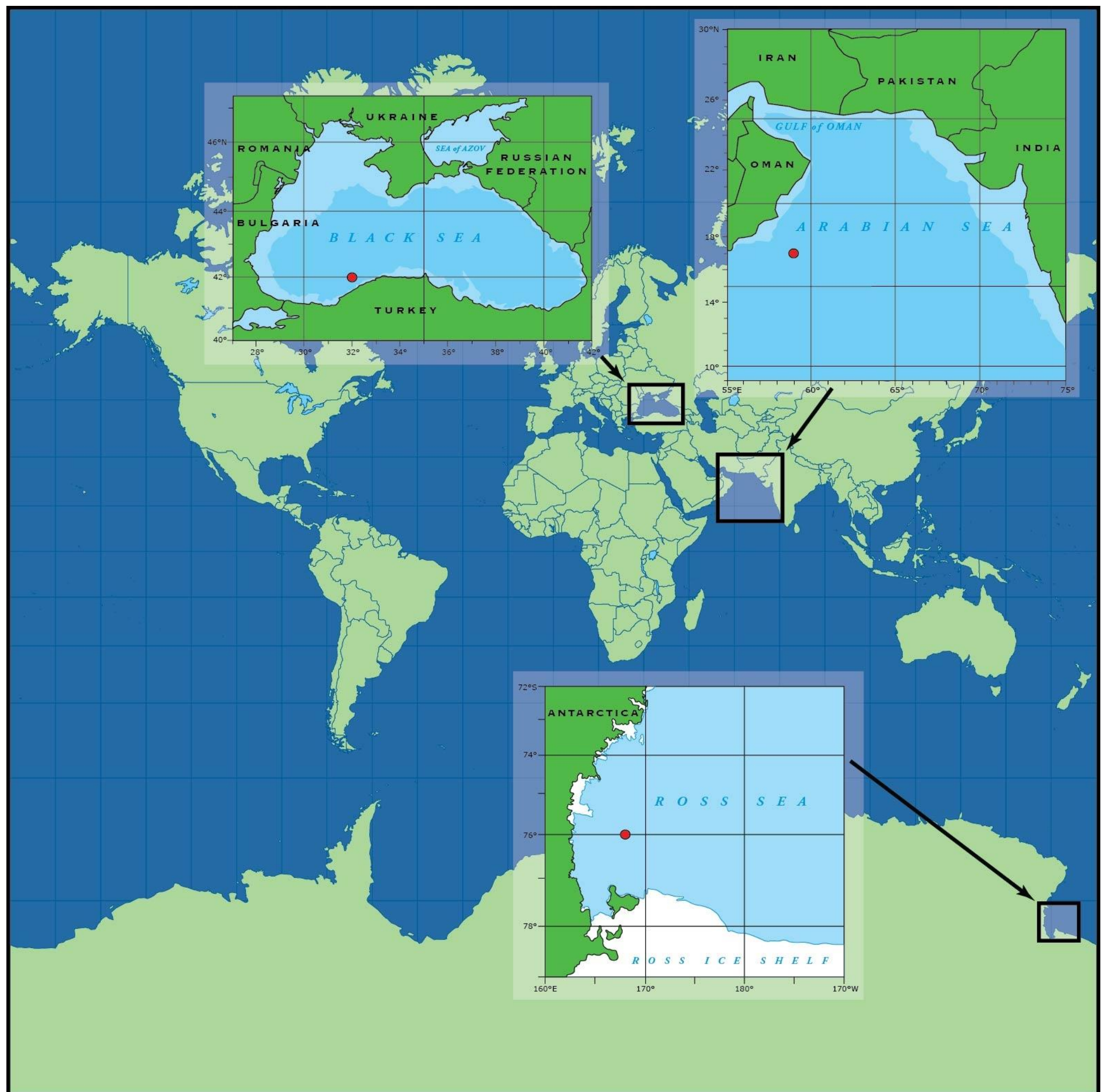


Figure 2

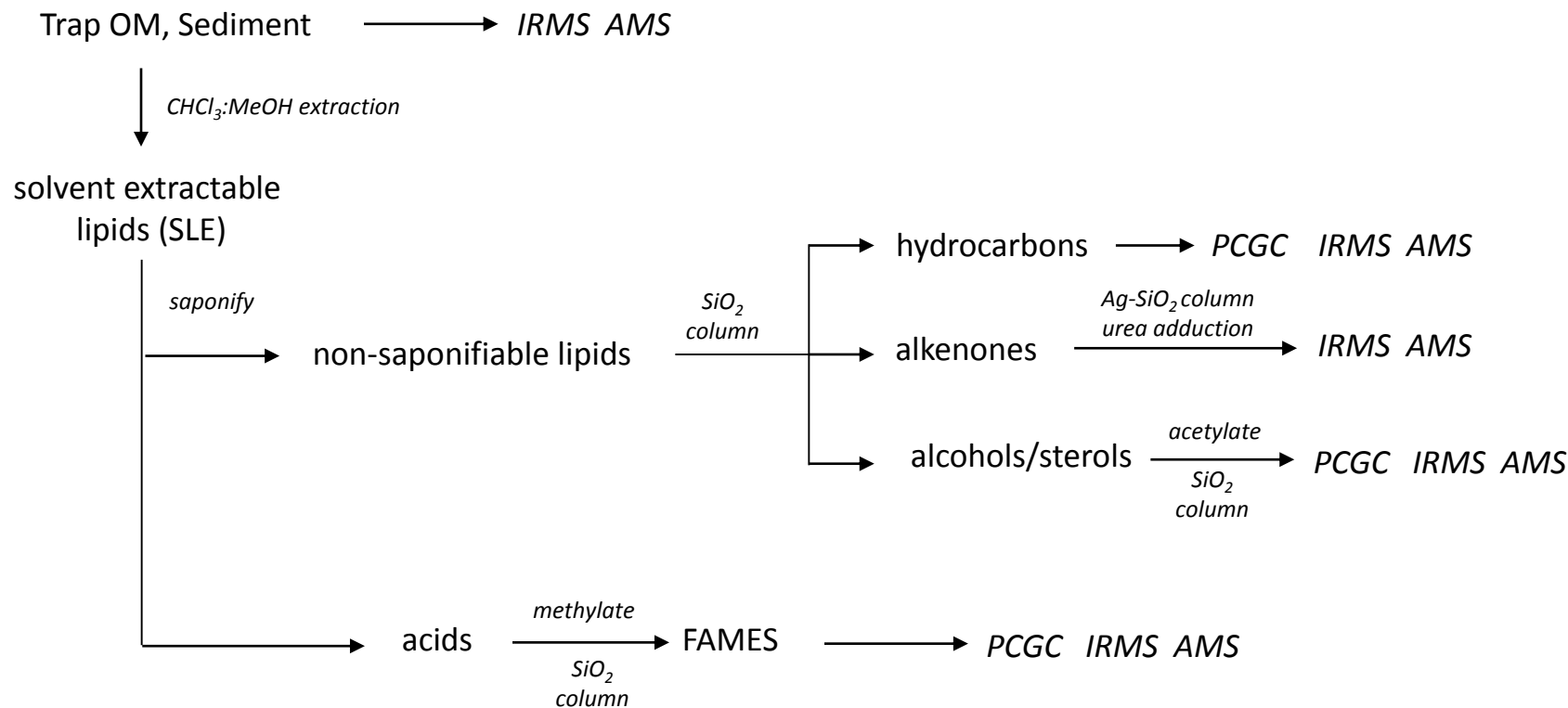


Figure 3

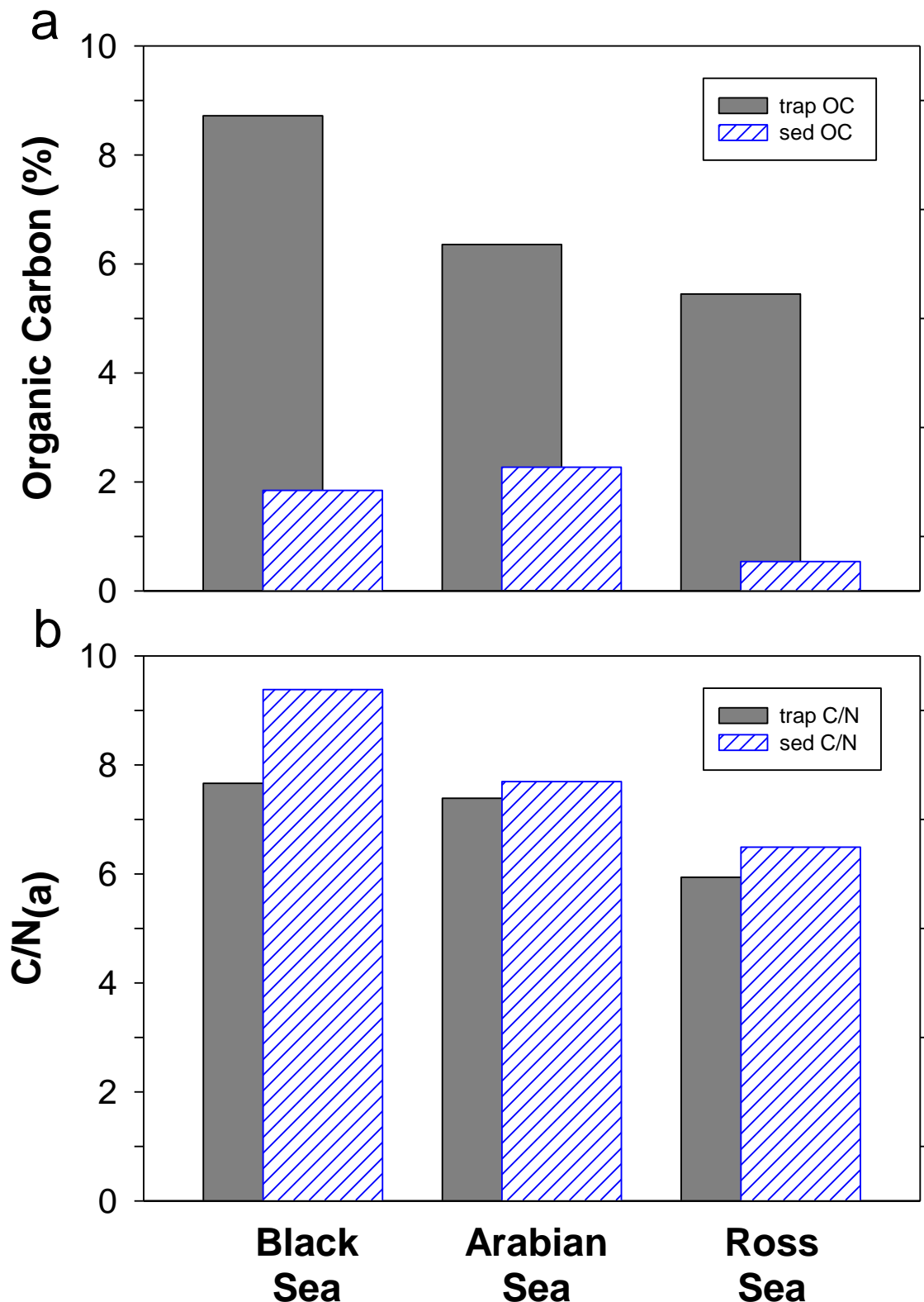


Figure 4

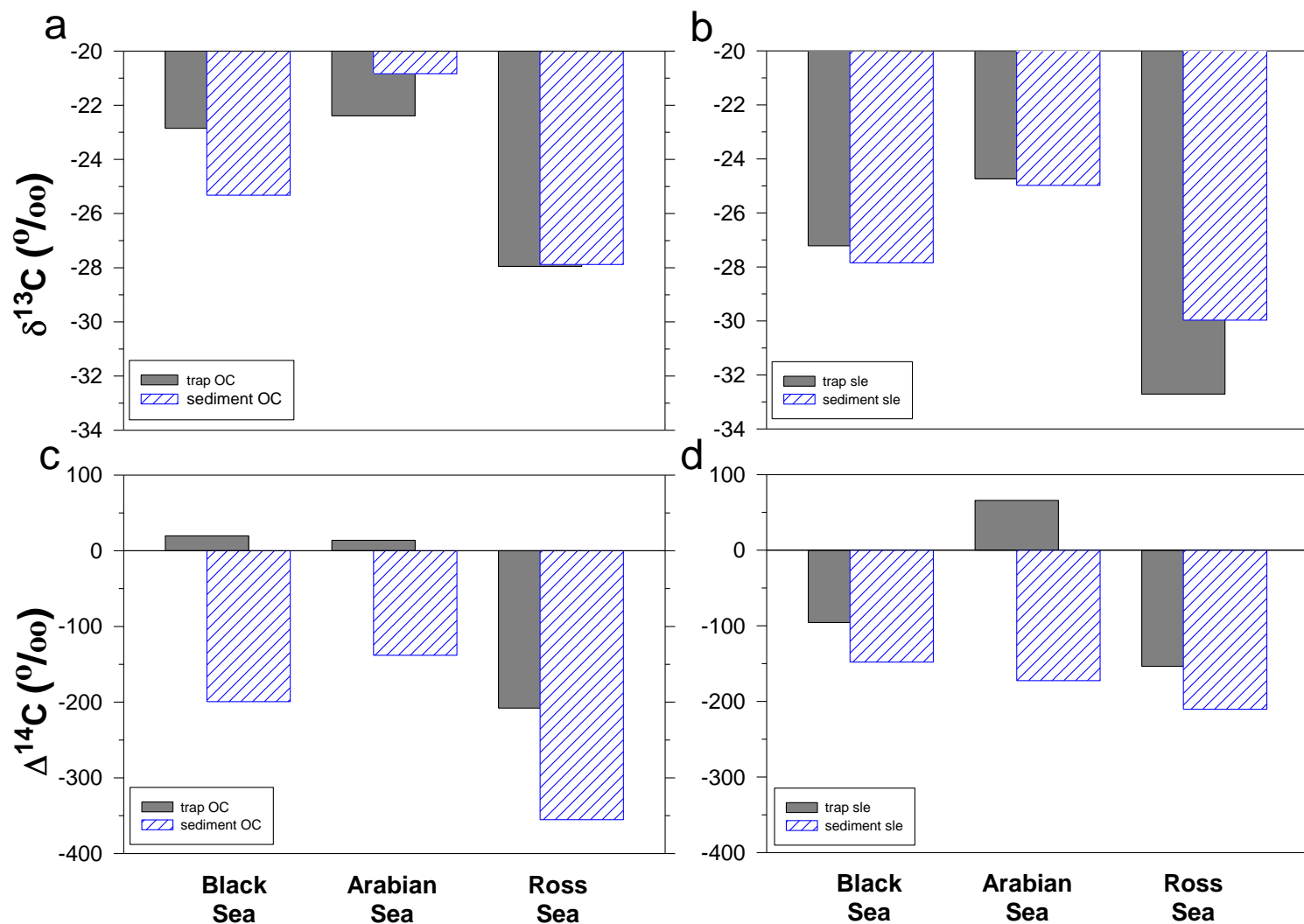


Figure 5

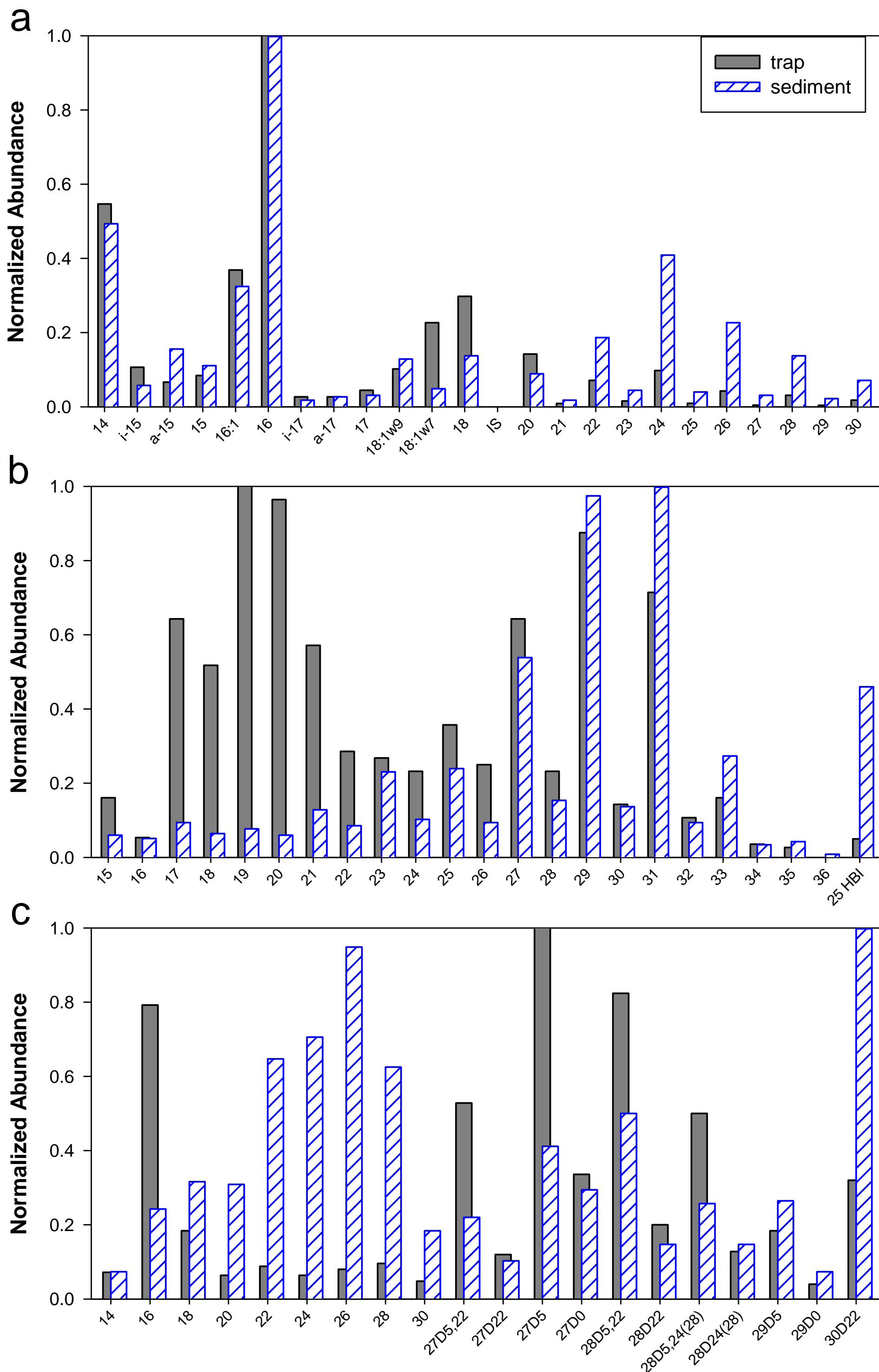


Figure 6

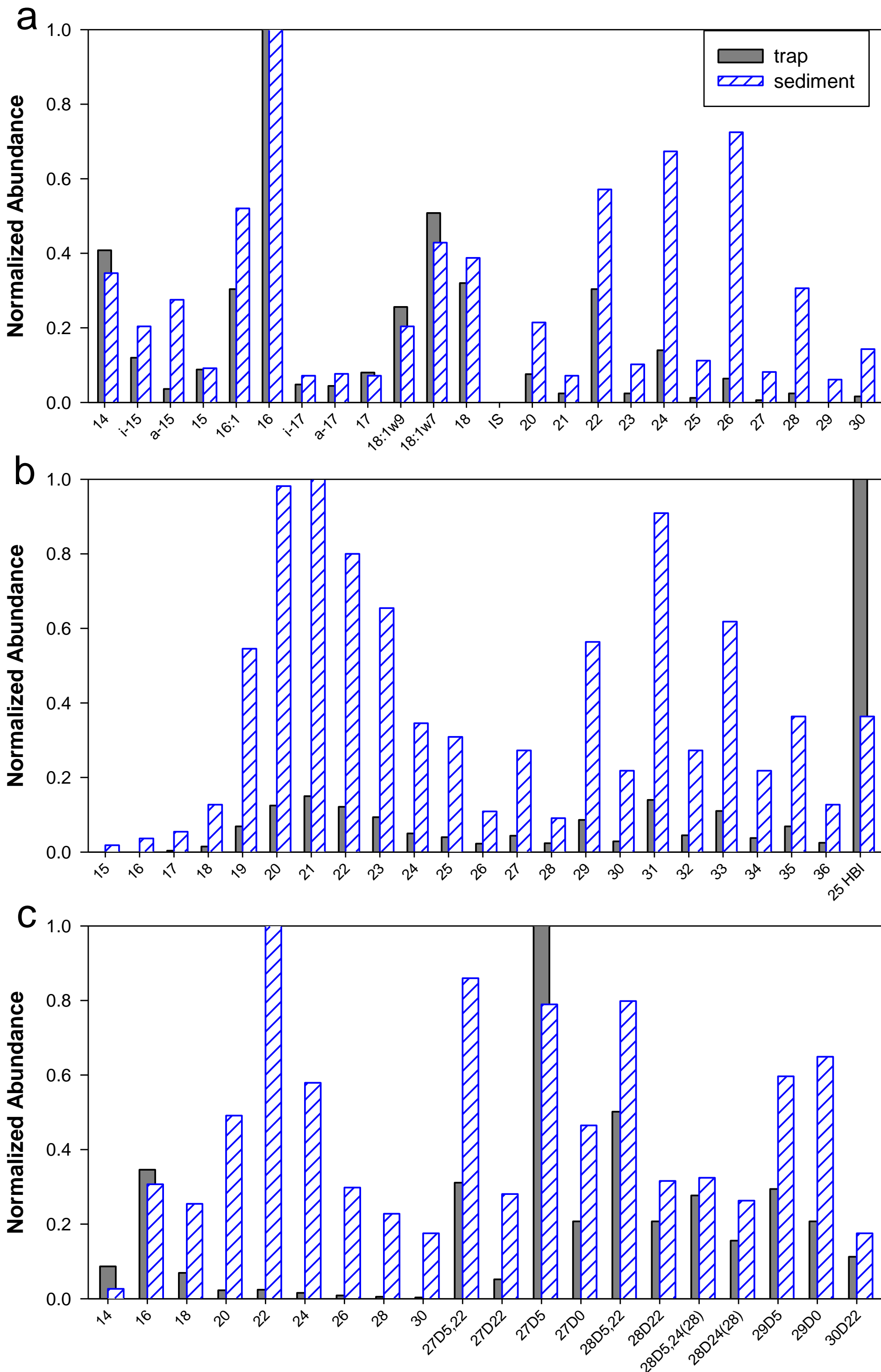


Figure 7

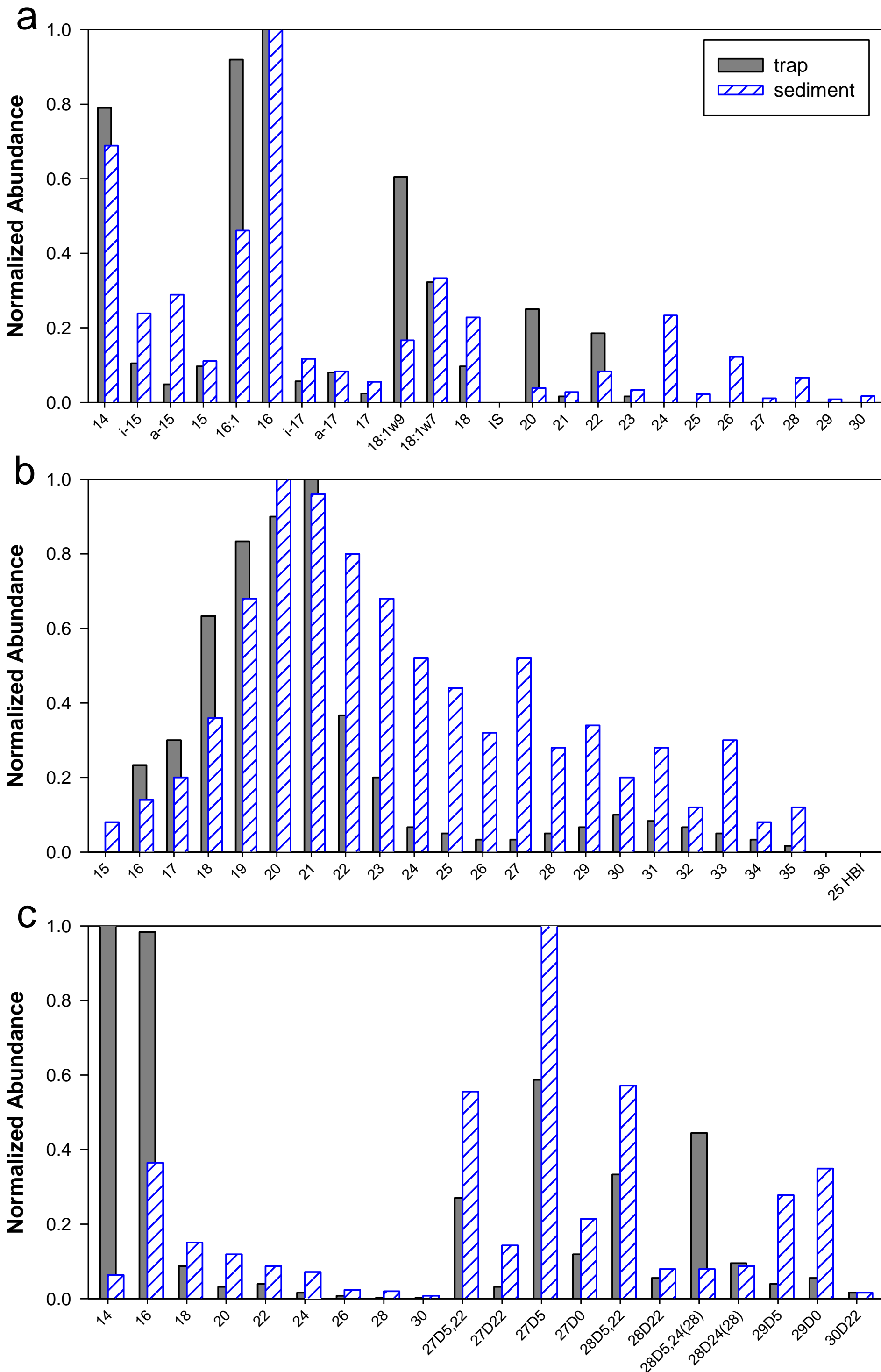


Figure 8

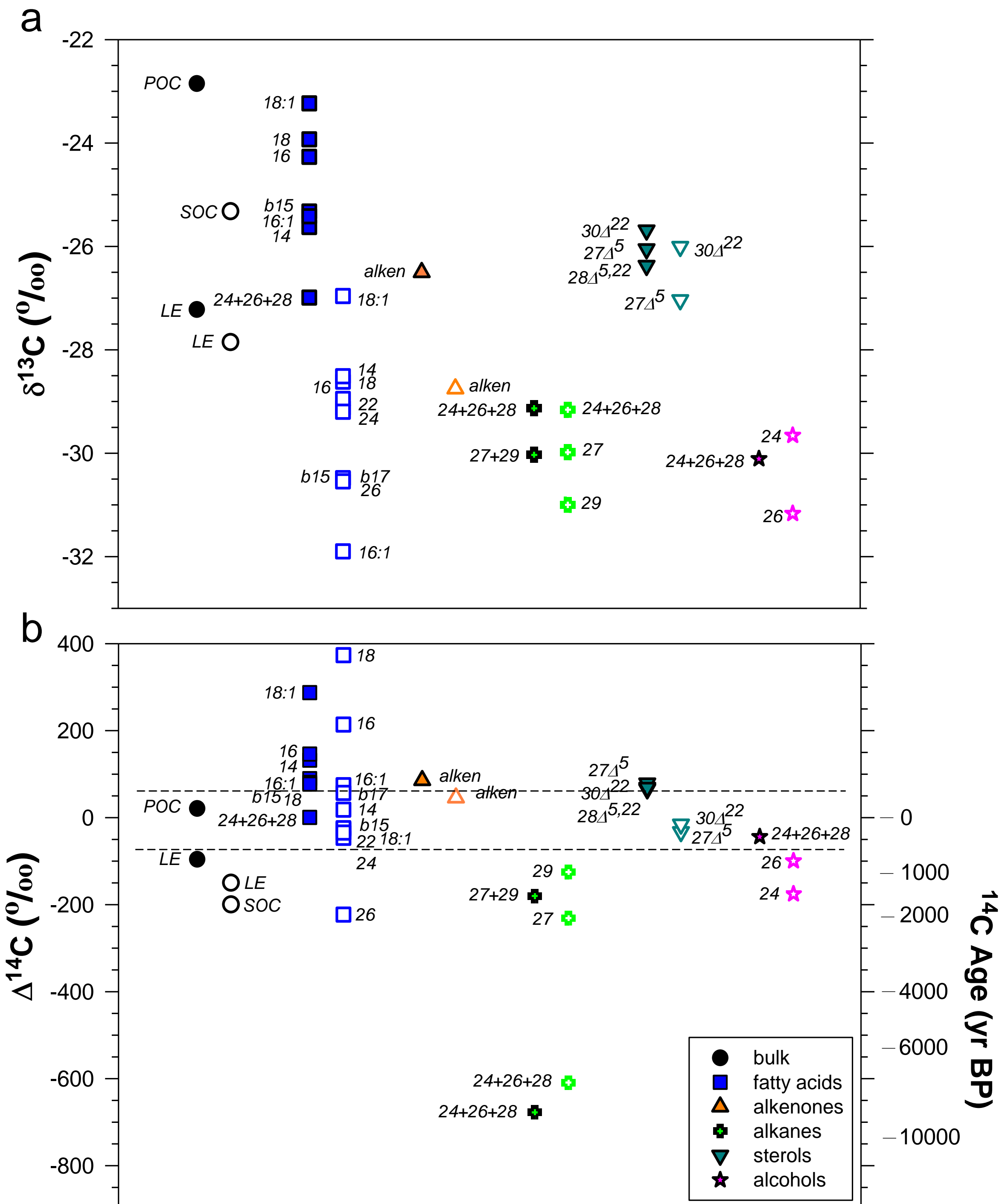


Figure 9

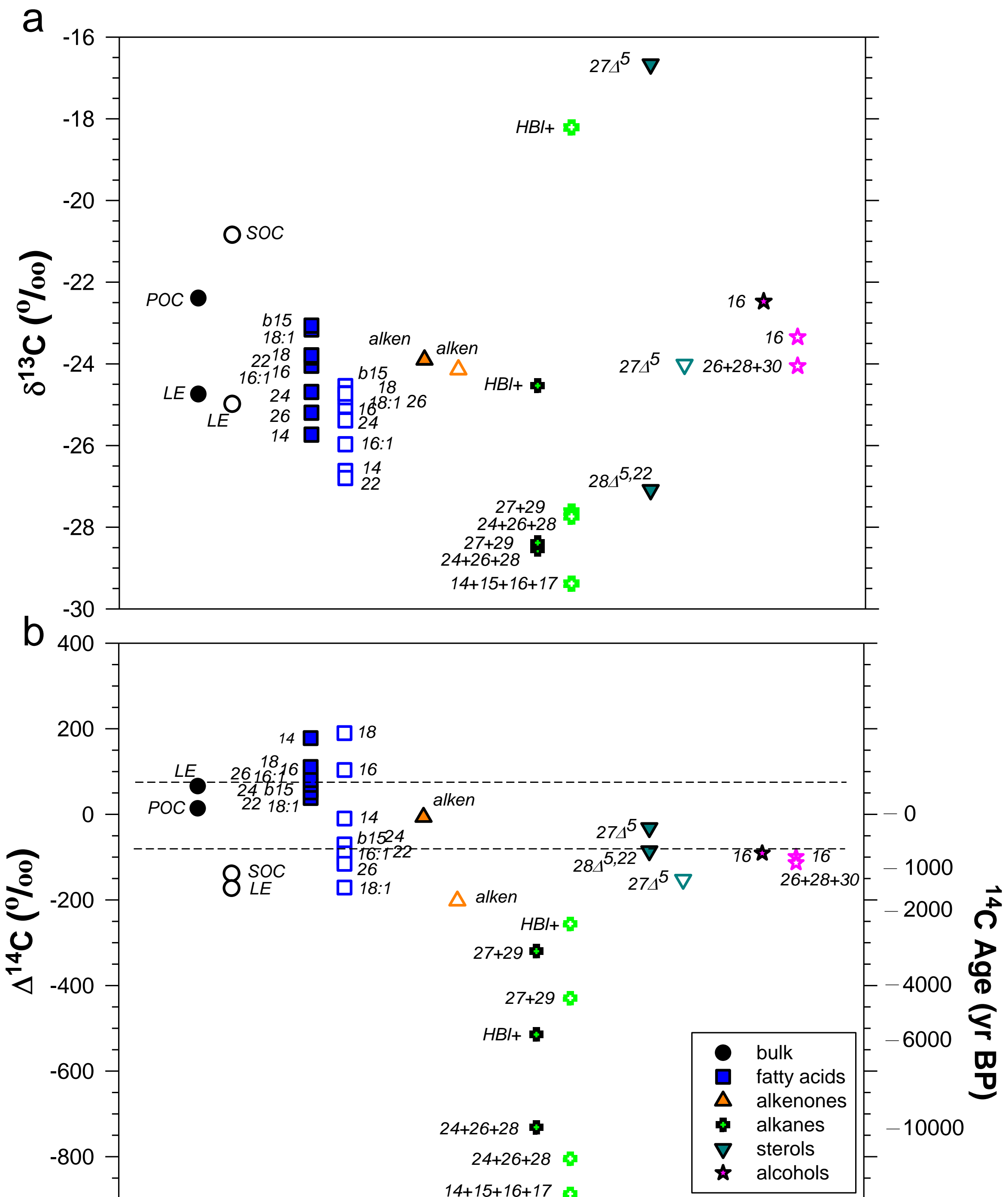


Figure 10

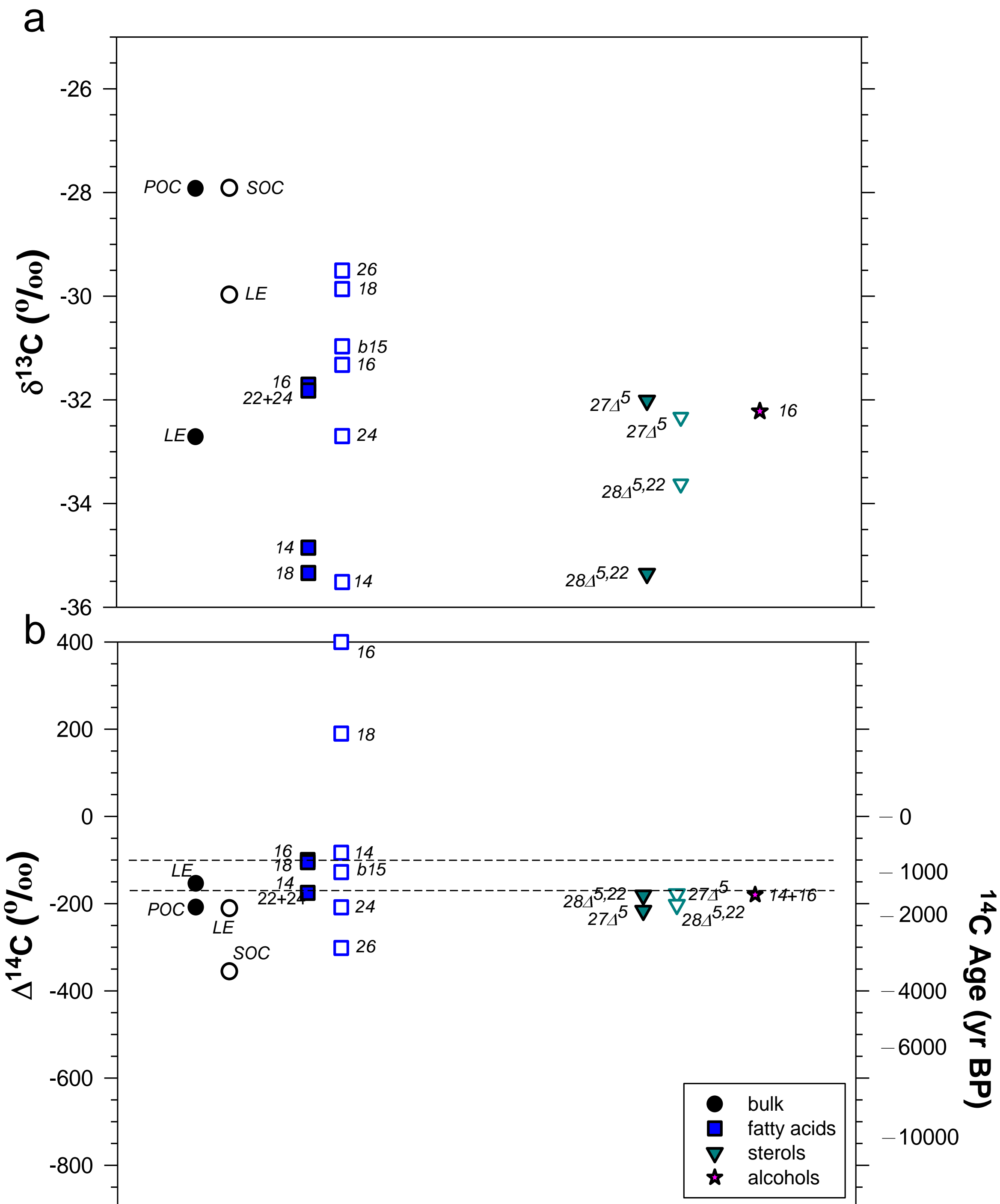


Figure 11

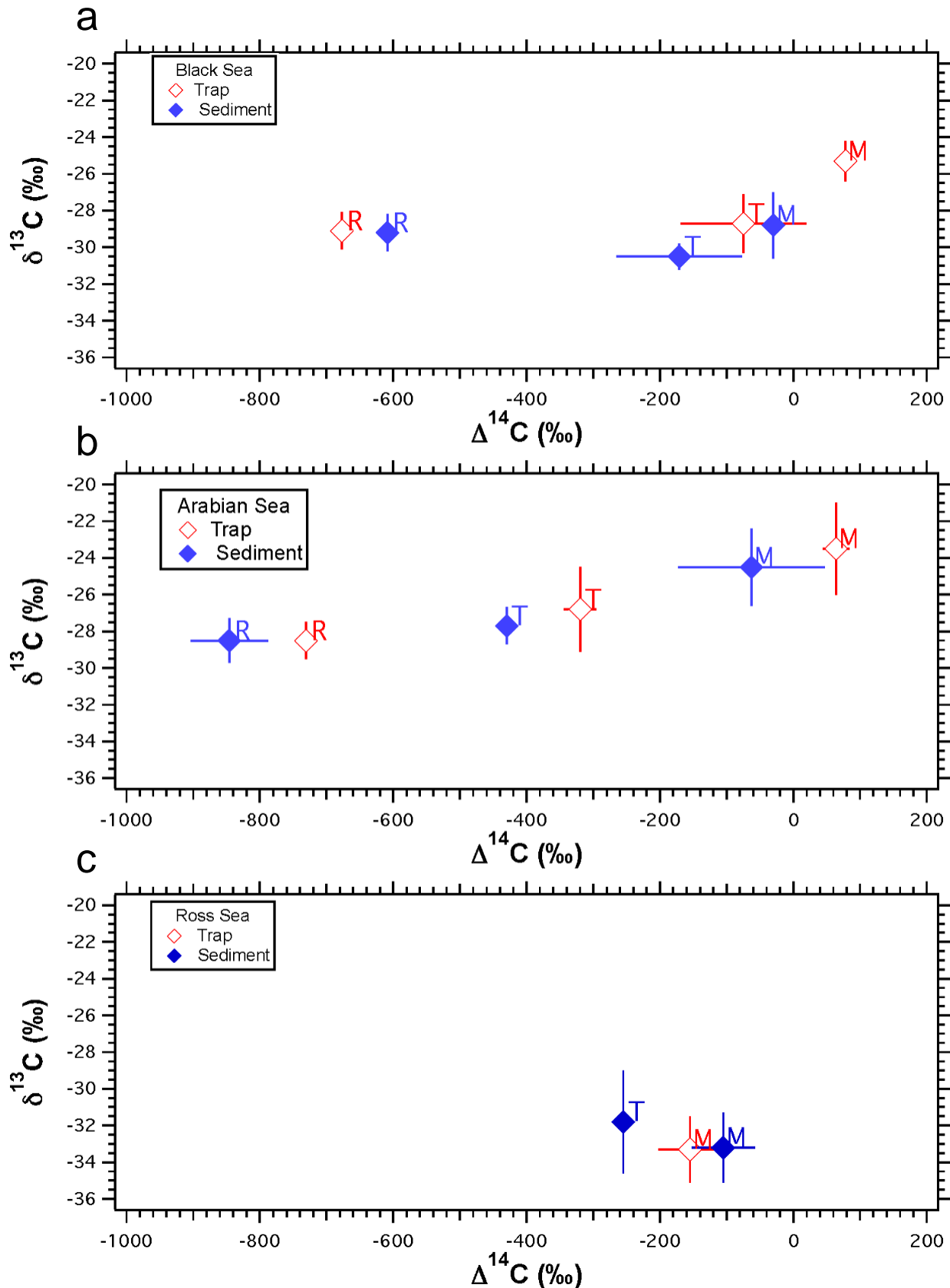


Figure 12

